DEVELOPMENT OF A TWO-WAY BREATHING RESPIRATOR WITH POLYMERIC ABSORPTION

C.E. Brown
K.M. Kalumuck
S. Prabhukumar
G.L. Chahine

March 1996

DYNAFLOW, INC.
7210 Pindell School Road
Fulton, MD 20759

The work described in this progress report was conducted under
SBIR Phase II Grant No. R44 OH03011-03 from the
National Institute of Occupational Safety and Health
Centers for Disease Control
Atlanta, GA
Principal Investigator: Clinton E. Brown

Contents

LIST OF ABBREVIATIONS

A	Frontal area of respirator filter
A_M	Diffusional area of membrane exchanger
ABACD	Abietic acid
C	Toxic gas concentration
C_a, C_p	Toxic gas concentration in air and in polymer
C_m	Time and space averaged toxic gas concentration exiting the respirator
C_{me}	Measured concentration in lag test
C_o	Toxic gas concentration entering the respirator air channels
c_a, c_p	Specific heat in air and polymer
D_a, D_p	Diffusion coefficient for air and polymer
DMS	Dimethyl-silicone
Fpol	Fluoropolyol
H	Heat of solution
k_a, k_p	Thermal conductivity in air and polymer
K	Partition coefficient, ratio of concentrations in polymer and air at equilibrium
L	Channel length
m_o	Weight of polymer in test unit
Δm	Added weight due to absorption of toxic gas
N	Relation defined by Equation (25)
p	Ambient air pressure
p_o	Air pressure at gas generator
p'_o	Vapor pressure at gas generator temperature
Q	Total volume flow rate through a respirator
r	Distance in radial direction
R	Gas constant for a particular gas
R_a	Channel radius
R_p	Effective radius of the polymer layer
S	Solubility of toxic gas in polymer
t	Time
t_c	Characteristic lag time
T	Temperature
T_o	Gas generator temperature
U	Velocity in the channels
U_A	Approach or apparent air velocity to the filter
U_{mean}	Time and space averaged velocity in the channels
x	Axial distance
y	Distance into the polymer
z	Half spacing distance of the channel holes
δ_p	Polymer membrane thickness
ε	Fraction of respirator frontal area occupied by air channels
μ	Viscosity of air
ρ_p	Polymer density
τ	Half the breathing cycle period

LIST OF FIGURES

LIST OF TABLES

SIGNIFICANT FINDINGS

The research conducted on two way breathing in respirators using polymeric absorption included both analytic and experimental studies and has led to the following major findings:

1. In a respirator filter using many parallel channels the reverse flow on outbreath can scavenge vapors absorbed on inbreath and provide substantial gains in breakthrough times relative to conventional one way absorption.

2. A state of equilibrium is reached in such a system so that no further increases in exiting concentration occur. The level of the exiting concentration is dependent on the geometry of the passages, length, diameter, spacing and number as well as the absorptive and diffusional characteristics of the polymer/gas pair involved.

3. Weight and size of the two way systems can compete with adsorptive activated charcoal under conditions for which the vapors to be filtered have low vapor pressures at room temperature and the polymer /gas pair have sufficiently high partitions coefficients.

4. Two way breathing produces in the filter bed a temperature distribution such that the air breathed is nearly at body temperature.

5. Two way flow respirator performance was found to be nonlinearly related to channel radius velocity and length. Doubling the length or halving the velocity or the radius resulted in order of magnitude increases in performance.

ABSTRACT

Experimental and analytical studies were made to predict the toxic gas removal capabilities of a respirator system using alternating flow (inhaling and exhaling) through a bed of absorbent polymeric material. For guidance in formulating experimental tests and for predictive purposes a numerical analysis was developed for a polymer bed composed of fine parallel channels. Mass and heat transfer computations were carried out to identify parameters having significant impact on the absorptive capacity of the system. For mass transfer, partition coefficients and diffusivities of the toxic gas polymer pair were found to be of primary performance as were the diameter, length and spacing of the channels. Air flow velocity in the channels also produced significant effects on performance. To corroborate the findings of the analyses a series of simulated breathing experiments were done in which oscillatory flow at typical breathing frequencies was passed through polymer test modules. The entering air contained measured concentrations of gases to be removed while the exhaust air had none. Concentrations of gas in the exiting air were measured as a function of time using flame ionization detectors. Both experiments and calculations found that the oscillating flow system reached an equilibrium state for which no further increases in exiting concentration occurred. Comparison of analytical and experimental predictions showed reasonable agreement and validated the analytical results.

Measurements of partition coefficients and permeabilities of various polymers were made for the gases Toluene and DiMethylMethyl-Phosphonate. Partition coefficients were found to vary from one polymer to another by orders of magnitude, and polymers tested showed significant sensitivity to temperature.

The temperature distribution in the oscillating flow respirator channel was found to rapidly approach nearly linear variation from the entrance to the exit with the exiting temperatures being essentially body temperature and outbreath temperature at the entrance being that of the ambient atmosphere.

The potential of oscillating flow respirators to compete with typical respirators using activated charcoal was evaluated for several cases in which the activated charcoal was assumed to be used in the usual one way flow arrangement. Oscillating flow polymer respirators were found to be competitive for gases at high percentages of saturation. Use in conjunction with supplemental air could greatly extend the life of the air supply.

1 Introduction

This report presents results of research carried out in an effort to improve workplace respirators by reductions in size and weight. The concept studied involves alternating flow (inhaling and exhaling) through the filter material allowing for ejection of a large fraction of the toxic material captured by the filter during intake. Systems using activated charcoal presently in use are valved because the charcoal degrades in adsorptive performance if exposed to humid breath on exhaling. Thus for two-way flow it is important to find filter materials that are not degraded by the presence of water vapor at concentrations found in human breath. To this end, the project concentrated on polymeric materials that *absorb* rather than *adsorb* toxic gases. To obtain the necessary mass transfer the polymeric material could be perforated by various means such as fine parallel holes, or the material could conceivably be formed of matted fine fibers or an open celled foam.

For guidance in planning and carrying out an experimental program, analytical studies were done for the case of polymers perforated with fine parallel holes. The differential equations representing the mass and heat transfer within the air channels and the polymer were solved numerically. Two special limit cases were also solved analytically. One assumes infinitely small sized perforations of the polymer, and the other considers the mass transfer after a final equilibrium has been attained. Both analyses provide useful information on the relationship between geometric and flow parameters.

Experimental studies of simulated breathing were made for various selected polymers made up into modules representing a small fraction of the face area of a potential respirator filter. Face velocities into the filter were cycled sinusoidally and the mean velocities as well as the breathing period were varied. The experimental work also included measurements of polymer gas pair partition coefficients and diffusivities as these physical parameters were found to be of primary importance and not available in the chemical literature.

Finally, engineering estimates were made to determine the weight and size of a conceptual oscillating flow respirator and comparisons were made against activated charcoal adsorption systems.

2 Analysis of the Mass and Thermal Transport

2.1 Basic Assumptions and Simplifications

In order to study the influence of various parameters, a model was formulated for the case of a respirator consisting of an array of small diameter cylindrical perforations in a polymer of some finite thickness. Such a configuration allows for an approximate computation of the mass and heat transfer between the air in the channels and the solid polymer. If we consider an arrangement of holes whose centers are arranged in an equilateral triangular grid as depicted in Figure 1, the respirator can be modeled as consisting of a large number of identical cells of hexagonal cross section in whose center is an air channel of circular cross section. The amount of polymer in each cell surrounding a channel can be written:

$$Polymer\ Volume = (2\sqrt{3}z^2 - \pi R_a^2)L \tag{1}$$

where z is one half the center to center hole spacing distance, L is the channel length and R_a is the channel radius. The first term in this expression is the area of the hexagonal cell while the second is simply the channel cross sectional area. To simplify the calculation with small error we consider the problem to be axially symmetric and introduce an effective radius R_p such that the polymer volume included in a cell of circular cross section with radius R_p surrounding the air channel of radius R_a is the same as that in the hexagonal cell. The defined radius, R_p, is given by the relation

$$\mathrm{R}_p = \left[\frac{2\sqrt{3}z^2}{\pi}\right]^{0.5}. \tag{2}$$

The flow of air into this system is characterized by two mean velocities, the mean velocity in the air channel, U_{mean}, and the mean apparent velocity, U_A. These velocities are related by the expression

$$U_{mean}\mathrm{R}_a^2 = \mathrm{U}_A\mathrm{R}_p^2, \tag{3}$$

where U_A is the velocity of the air approaching the filter. The air velocity must, of course, speed up as it enters the polymer channels.

Other simplifications of the analysis are the assumption that thermal conductivity and specific heat of the polymer are independent of toxic gas concentration. However, we do include variation with temperature of the properties governing the absorption, desorption, and diffusion of the contaminant gas. The solubility and partition coefficient are particularly sensitive to temperature. For example, in [1] it was found that the solubility and partition coefficients for various polymers can vary by more than a factor of 3 over the temperature range $30°C$ - $50°C$. We have found the same trends in our measurements. Thus the instantaneous temperature distribution in the respirator could be important to properly model the absorption, desorption and transport of the contaminant gas. To this end we developed a coupled heat and mass transfer model to predict system performance. The model solves the heat and mass transport equations for fully developed laminar flow[1] in polymer tubes. The heat and mass transfer transport relations are coupled due to the temperature dependence of various properties as described below.

The parameters of the model problem as sketched in Figure 2 include:

(a) the polymer/gas pair partition coefficient, K,

(b) the mass diffusion coefficients of the gas in the air and in the polymer, D_a, D_p.

(c) the physical dimensions: tube radius, length and radius of the outer boundary of the polymer layer, R_a, L, R,

(d) the axial flow velocity, U,

(e) the concentrations of gas in the air and polymer, C_a, C_p,

(f) the air and polymer temperatures, T_a, T_p,

(g) the air and polymer densities, ρ_a, ρ_p,

[1]The Reynolds number based on mean air flow velocity and tube diameter is of the order of 1-2 for typical conditions in the respirator.

(h) the air and polymer thermal conductivities and specific heats. k_a, k_p, $c_{p,a}$, $c_{p,p}$.

The axial velocity distribution in the channel can be written

$$U(x,r,t) = U_{mean} \cdot f_1(r) \cdot f_2(t) \cdot f_3(x,t), \tag{4}$$

where U_{mean} is the uniform velocity entering the tube averaged over one half a breathing cycle, τ, x and r are axial and radial coordinates and t is time. Here,

$$f_1 = 2(1 - \frac{r^2}{R_a^2}), \tag{5}$$

$$f_2 = \frac{\pi}{2}\sin(\pi\frac{t}{\tau}), \tag{6}$$

and

$$f_3 = \frac{T_a(x,0,t)}{T_a(0,0,0)}. \tag{7}$$

Equation (5) represents a laminar and fully developed flow. This assumption is justified by order 1 Reynolds numbers to be considered in the calculations. Equation (6) is an approximation to human breathing cycles. Typical values for τ are 2.5 seconds for in breath and 3.5 seconds for out breath. Equation (7) allows for mean density change along the tube produced by the axial temperature variation at the tube centerline $T_a(x,0,t)$ (which approximates well the bulk mean temperature within the channel at any station x since as will be seen later, radial gradients in air temperature are negligible). $T_a(0,0,0)$ is the air temperature on entering the tube. The velocity distribution within the tube is then

$$U(x,r,t) = \pi U_{mean}\sin\frac{\pi t}{\tau}(1 - \frac{r^2}{R_a^2})\frac{T_a(x,0,t)}{T_a(0,0,0)}. \tag{8}$$

2.2 Thermal Transport

The thermal transport equations can then be expressed as

$$\rho_a c_{p,a}\frac{\partial T_a}{\partial t} = \frac{\partial k_a}{\partial T}\nabla T_a + k_a\nabla^2 T_a - \rho_a U c_{p,a}\frac{\partial T_a}{\partial x}, \tag{9}$$

$$\rho_p c_{p,p}\frac{\partial T_p}{\partial t} = \frac{\partial k_p}{\partial T}\nabla T_p + k_p\nabla^2 T_p, \tag{10}$$

where subscripts a and p refer to the air and polymer. The boundary conditions include a specified known temperature at the inlet for both the forward and reverse flows. At the polymer/air interface, ($r = R_a$), the conditions are continuity of heat flux and of temperature

$$k_a\frac{\partial T_a}{\partial r} + h_{sol}D_a\frac{\partial C_a}{\partial r} = k_p\frac{\partial T_p}{\partial r}, \qquad r = R_a. \tag{11}$$

$$T_a = T_p, \qquad r = R_a, \tag{12}$$

where k_a and k_p are the thermal conductivities of the air and polymer, and h_{sol} is the heat of solution for the gas forming a solution with the polymer. Selection of the boundary condition at the outer edge of the polymer depends on the actual physical geometry as previously discussed. In a multi tube respirator, the boundary between the polymer layers associated with adjacent tubes can be modeled as having no net transfer across them since all tubes are taken as being identical. Thus the boundary condition at $r = R_p$ is:

$$\frac{\partial T_p}{\partial r} = 0, \qquad r = R_p. \tag{13}$$

(14)

The outer face of the polymer respirator is in contact with atmospheric air and the inner face is in contact with the region of air near the mouth. The heat transfer across these boundaries is negligible as it must occur through radiation or conduction to stagnant air. and the boundary condition can be approximated as being adiabatic:

$$\frac{\partial T_p}{\partial x} = 0; \qquad x = 0, L. \tag{15}$$

At the air channel entrance ($x = 0$) during inbreath the temperature is equal to atmospheric temperature. During outbreath the air temperature at the mouth ($x = L$) is equal to that of the exhaled air. The outflow conditions for both the forward and reverse flows are taken to be:

$$\frac{\partial T_a}{\partial x} = 0 \text{ at } x = L,\ U > 0;\ \text{and } x = 0,\ U < 0. \tag{16}$$

2.3 Mass Transport

In situations where the bulk fluid density ρ is not constant, such as will be the case in the air channel with varying temperature, it is convenient to express the equations in terms of a mass fraction C_a^* where

$$C_a^* = \frac{C_a}{\rho}. \tag{17}$$

Due to a very low coefficient of thermal expansion (e.g., for DiMethyl Silicone - DMS - the density variation over the temperature range $17°C$ to $37°C$ is less than 1% of its mean value) the polymer density is taken as constant. The differential equations governing the mass transfer in axisymmetric geometry are then:

$$\rho_a \frac{\partial C_a^*}{\partial t} = \frac{1}{r}\frac{\partial}{\partial r}(r\rho_a D_a \frac{\partial C_a^*}{\partial r}) + \frac{\partial}{\partial x}(\rho_a D_a \frac{\partial C_a^*}{\partial x}) - \rho_a U \frac{\partial C_a^*}{\partial x}, \tag{18}$$

$$\frac{\partial C_p}{\partial t} = \frac{1}{r}\frac{\partial}{\partial r}(r D_p \frac{\partial C_p}{\partial r}) + \frac{\partial}{\partial x}(D_p \frac{\partial C_p}{\partial x}). \tag{19}$$

The boundary conditions at the polymer/air interface are:

$$D_a \frac{\partial C_a}{\partial r} = D_p \frac{\partial C_p}{\partial r} \text{ at } r = R_a, \tag{20}$$

$$C_p = KC_a \text{ at } r = R_a. \tag{21}$$

At the polymer outer boundaries, by the same argument used for the thermal problem:

$$D_p \frac{\partial C_p}{\partial r} = 0 \text{ at } r = R_p;\ x = 0, L. \tag{22}$$

In the air channel, at in-flow, the upstream concentration is equal to the initial concentration, and on reverse flow the return concentration is zero. The outflow conditions for both the forward and reverse flows are taken to be $\frac{\partial C_a}{\partial x} = 0$, at $x = L$, $U > 0$; and $x = 0$, $U < 0$.

2.4 Numerical Implementation

An Alternating Direction Implicit (ADI) finite difference scheme [2] was developed to solve the problem of flow of air through a polymer lined tube, which included the following:

a) unsteady diffusion and convection of both heat and mass,

b) simultaneous heat and mass transfer with an imposed time dependent temperature boundary condition and velocity profile.

c) temperature dependent air and polymer properties, and

d) heat of solution effects (heating/cooling effects due to mass absorption/desorption).

The ADI was implemented utilizing second order centered differences in space and first order forward differences in time. Second order accurate boundary conditions were employed except at the air/polymer interface where, for increased accuracy, a fourth order scheme was employed. The ADI was chosen over other schemes for reasons of stability and speed [2] For the problem at hand which involves a combination of diffusion, convection, and interface boundary conditions that couple the polymer and the air channel, it was found that a criterion for stability established a maximum allowable time step.

A series of stability and convergence studies were performed which led to the following stability criterion:

$$D_a \Delta t/(\Delta r)^2 \leq 2, \tag{23}$$

where Δr and Δt are the space and time step sizes. This is a factor of 8 increase in the maximum allowable time step over the explicit method of solution utilized in Phase I [3].

A detailed convergence analysis was performed to establish the sensitivity of the code to space and time discretization size. Properties of the polymer gas pair Dimethyl Silicone and Dimethyl Methyl Phosphonate (DMMP) that we measured were used. It was found that results were very sensitive to resolution of the behavior at the air/polymer interface. The temperature and concentration gradients must be adequately resolved to accurately compute the heat and mass transfer across this interface. The fourth order difference scheme used at the interface was found to achieve a high degree of accuracy with a reasonable discretization.

Figure 3 shows plots of the nondimensional concentration (C_a/C_o) versus x in the air channel center line ($r = 0$) and versus r at $x/L = 0.8$. All figures are at the end of the first forward flow (inbreath) cycle. *The concentration inside the polymer is normalized using the*

partition coefficient, K, to enable the concentrations in the air and the polymer to be displayed on the same scale. In Figure 3a, the discretizations in the r-direction and in time were held constant. The discretizations in the axial direction were reduced from 75 grid points (nx) down to 5 with little difference in the results. These figures show the insensitivity of the results to the axial discretization. In Figure 3b, the radial and temporal discretizations were varied. The axial discretization was also varied to maintain the same grid aspect ratio. It was not possible to analyze the discretizations in the r-direction and in time separately because of the stability criterion discussed earlier. Stability considerations forced a decrease in the time step with a decrease in the grid size.

Based on these results a discretization of 20 points in both the axial and radial directions with a time step of $5 \cdot 10^{-3}$s was chosen as adequate for providing a converged solution.

2.5 Long Time Equilibrium Conditions

The oscillatory flow through the polymer absorber leads to an equilibrium state at long times for which no further changes occur in the mean concentration of the inhaled air. Analysis of this special case has been made and is presented in detail in Appendix A. The solution for the equilibrium value of the exiting mean concentration, C_m, is given by the expressions:

$$\frac{C_m}{C_o} = \frac{N}{1+2N}, \tag{24}$$

where

$$N = [\frac{1}{2K}\sqrt{\frac{\pi\tau}{D_p}} + \frac{0.719 \cdot R_a}{D_a} + \frac{8 \cdot D_a}{\pi R_a U_{mean}^2}]\frac{\pi R_a U_{mean}}{4L}. \tag{25}$$

Comparisons of the results of the analysis has been made with the results of the numerical code and are presented in the following table:

TABLE 1: EQUILIBRIUM ANALYSIS COMPARISON

U_{mean}	K	R_a	L	D_p	D_a	2τ	C_m/C_o	C_m/C_o
cm/sec		cm	cm	cm^2/sec	cm^2/sec	sec	Numerical	Eq(24)
12.2	8000	0.0254	1.27	2×10^{-7}	0.075	6	0.104	0.102
12.2	11700	0.0254	1.27	2×10^{-7}	0.075	6	0.090	0.084
3.72	8000	0.0794	1.27	2×10^{-7}	0.075	6	0.18	0.166
3.72	11700	0.0794	1.27	2×10^{-7}	0.075	6	0.17	0.154
3.72	8000	0.0794	1.27	2×10^{-7}	0.0375	6	0.27	0.213

There is quite reasonable agreement between the two calculation methods at least at the low values of C_m/C_o that are of interest for respirator applications. The analysis provides an independent check on the numerical code and can be used for quick approximate estimation of the long time effects of changing parameters. It. however, does not predict the short term behavior.

2.6 Limiting Solutions for Infinitesimal Hole Size

It is of interest to determine the absorber performance that could be achieved by reducing the hole sizes in the polymer to zero while keeping the ratio r_p/r_a constant. This would provide for maximum (in fact infinite) radial mass and heat transfer in the air and polymer. It thus represents an upper bound on the performance that could be achieved by decreasing air passage size. The problem is than one-dimensional in space - a function only of position x. A numerical analysis of this case was made for the case of constant diffusivity and partition coefficient. The assumed small zero scale of the lateral dimensions ensures that the air and polymer concentrations will be independent of r, that is, the mass transfer over the assumed small radial distance is so fast that equilibrium is achieved. The differential equation to be solved becomes:

$$\frac{\partial C}{\partial t} = \left[D_p + \frac{D_a}{K(\frac{r_p^2}{r_a^2} - 1)} \right] \frac{\partial^2 C}{\partial x^2} - \frac{U_m}{K(\frac{r_p^2}{r_a^2} - 1)} \frac{dC}{dx}. \tag{26}$$

Note that the concentration is only a function of x and that in the polymer is K times that in the air channel. Boundary conditions at x = 0 and x = L are the same as those used for the complete problem above.

2.7 Computational Results

2.7.1 Preliminary Considerations

Calculations were carried out to obtain the estimated mean concentration exiting the tubes as a function of time. In respirator use its value must not be permitted to exceed some allowable concentration that depends on the toxicity of the compound. This "threshold limit value," TLV, is tabulated for most common chemicals. For a given TLV and an ambient concentration of toxic gas, C_o, the ratio C_m/C_o is determined and fixes the performance required of the respirator [4] as the time at which the exiting concentration exceeds the TLV and therefore the design value of C_m/C_o. For highly toxic compounds such as Sarin, a nerve gas, values of 0.001 or lower may be required whereas a less toxic compound, Toluene, may only require a C_m/C_o value at breakthrough of 0.01 or more. Obviously, the C_m/C_o value will depend on the estimated ambient concentrations which may range from traces to fully saturated conditions. The breakthrough-time and the required value of C_m/C_o determine the quality of the system and together with the polymer absorption characteristics will ultimately determine the size and weight of the respirator. The variables available for the design include the length of the polymer channels, the diameter of the channels and their spacing. The face area of the filter is proportional to the volume flow rate required for breathing and inversely proportional to the apparent velocity U_A previously discussed. To illustrate the effect of the several variables, runs were made varying only a single variable over what were considered reasonable values; for example, tube lengths of one half to two inches. As will be discussed later these lengths were considered to bracket values usable in a respirator application.

2.7.2 Partition Coefficient Effects

The variable of greatest interest is the partition coefficient, K, as this value for various polymer/gas pairs can vary from about 10^2 to 10^6; the lower values corresponding to gases having very high vapor pressures at room temperatures with the higher values corresponding to gases with low room temperature vapor pressures. The effect of partition coefficient variation is shown in Figure 4. The other parameters held constant are also shown on the figure. Note that for low K values the system arrives at an equilibrium state for C_m/C_o in a quite short time but for the large K values, equilibrium is delayed greatly. For respirator use, times less than an hour would be of interest for emergency use. For industrial use, two to eight hours would be desired. For larger values of the channel length, lower apparent velocities and smaller channel radii, the time to reach breakthrough values will be increased as will be shown in subsequent figures. The value of K of 80,000 shown in the figure may indeed be obtained for polymers absorbing low vapor pressure toxic compounds. The geometries shown would allow for breakthrough times as long as 10 hours for a C_m/C_o value of .01 and 4 1/2 hours for a C_m/C_o values of .001. An estimated weight for such a polymer filter is 95 grams. Further discussion of the respirator design will be found in Section 5.

2.7.3 Geometry Effects

Variation of the length and diameter of the passages has a major effect on the absorptive time histories. Figure 5 shows the result of length variation. Note that doubling the length doubles the amount of polymer involved in the mass exchange and this in turn provides a more than proportional reduction in the exiting concentration at any given time; e.g., a factor of 100 after 4 hours. Decreasing the channel radius, as shown in Figure 6, also produces marked reductions in exiting concentrations. Clearly the reduced diffusional distances play a major role in the overall mass transport. Of course in respirator considerations the pressure drop across the respirator, determined by hole size and length, is important and discussed further in Chapter 5. Figure 7 presents the results obtained in the limiting case of R_a approaching zero. Comparison with the results of Figure 4 indicates the importance in the respirator design of reducing the channel radius to values limited by the pressure loss in breathing. The curves shown for the longer 5.08 cm. channel lengths show that for this case the effect of the mean velocity is small. This effect is not borne out at a finite value of R_a as can be seen in Figure 8 where a favorable effect is shown for reduced apparent velocities. These limiting cases for R_a equal to zero are rather extreme in that the actual radial distances required under the assumptions must be extremely small because all the polymer is assumed to be reached by diffusion in the time period of breathing, 4 to 7 seconds.

The spacing of the holes in the perforated polymer sheet has a pronounced effect during the early times before approaching equilibrium as seen in Figure 9. Increased hole spacing (increased R_p/R_a) lengthens the time to equilibrium improving performance substantially at times of a few hours. The improvement is accompanied with a reduction in the apparent velocity which as will be seen later would entail increased weight of the respirator filter. Note that the spacing of holes affects the final specific gravity of the polymer filter. Obviously as the relative hole volume increases the polymer matrix become less dense reducing the total filter weight, other factors being unchanged.

2.7.4 Diffusion Coefficient Effects

Diffusion in the polymer and air also play important roles in the performance of the respirator system. Figure 10 shows the result of variations in the polymer/gas diffusivity. Polymer diffusivities are not a design choice except by choice of the polymer. Values of polymer diffusivity can vary from 10^{-6} cm^2/sec to more than 10^{-10} cm^2/sec. Intuitively, the higher values of diffusivity should result in reduced vales of C_m/C_o as the gas can more readily diffuse to the outer reaches of the polymer. This is indeed seen in the figure.

Figure 11 demonstrates for the parameters shown a modest effect of the diffusion coefficient of the toxic gas in air. As the diffusivity in the air decreases, increased resistance to diffusion across the channel impairs absorption by the polymer. This also is not a variable that can be chosen but is only dependent on the diffusing gas.

2.7.5 Temperature Distribution

We examined the effects of temperature variation in the respirator which lead to variation in property values. Because the conduction of heat in the polymer is more rapid than diffusion the temperatures in the system reach equilibrium values relatively quickly as can be seen in Figure 12. The calculations used estimated values for polymer conductivity and specific heat and indicate an approach to an equilibrium state after only 12.5 minutes of breathing. There is, however, a very small temperature swing at any point in the channel during a breathing cycle as shown in Figure 13. For breath exhausting at 35°C and ambient air temperature of 20°C, the internal variation at any point is less than about three quarters of a degree centigrade. The resulting temperature distribution after only a short time shows that the air breathed would be at a temperature very close to body temperature, 37°C. Because of water vapor absorption, it can be expected that the breathed air would also contain a near saturated amount of water vapor. Whether this situation would be desirable for a respirator wearer is not clear at this time. For those persons with colds and clogged noses such a situation may assist in preventing excessive mouth and throat dryness.

2.7.6 Effect of Temperature Gradients on Mass Transfer

The effect of the temperature variation in the channel produced by breathing is illustrated by Figure 14 that shows one computation made with the temperature gradient effects included and a second computation for which the partition coefficients and diffusivities were held constant but chosen at the mean temperature level in the channel. The difference between the two computations is not great and indicates that simpler and less time consuming computations using the input variables at the mean temperature in the channel should be adequate for engineering design and evaluation of the respirator performance. Closer agreement for the two cases would result if the constant property values were selected at temperatures somewhat above the mean values.

2.7.7 Axial Concentration Distribution

Figure 15 presents the predicted concentrations along the channel axis as a function of time. The concave shape of the curves gradually approaches at long times a nearly linear variation

from the entrance to the exit of the channels. This result was used as the basis for the approximate closed form analysis presented in section 2.5. Figure 16 shows timewise variations in concentration at three radial positions at an axial station. It can be seen that the oscillations in concentration die out rapidly with radial distance into the polymer. It is not surprising that this is so as a one dimensional analysis of a sinusoidally varying concentration at the air polymer interface indicates that the amplitude of the diffusional oscillations should die out in the polymer according to the simple relation

$$C(y) = C_B \cdot e^{-\sqrt{\frac{\pi}{2\tau D_p}}y}, \tag{27}$$

where C_B is the amplitude of the concentration at the surface, y is the distance from the surface into the polymer, τ is the half period of the oscillation and D_p is the polymer diffusion coefficient. Considering a typical breathing period, 2τ, of six seconds and a diffusion coefficient of say 10^{-7} cm^2/sec the above relation shows that the penetration into the polymer to a concentration level of one percent of C_B would be only .0018 cm, which corresponds to a value in Figure 16 of $r/R_a = 1.073$. The small fluctuations at this depth would not be observable at the scale of the figure and the steady level shown here is the result of a continuous diffusion from the time mean values in the air channel. Thus as time proceeds concentrations in the outer regions of polymer grow steadily to reach an equilibrium value only dependent on distance along the channel. Thus any dependence on the ratio R_p/R_a vanishes as seen in Figure 9.

3 Experimental Methods and Results

Two classes of experiments have been conducted, polymer gas property measurements and simulated breathing experiments. Two gases have been used, DiMethyl MethylPhosphonate (DMMP) and Toluene having vapor pressures at room temperature of 1 and 20 Torr respectively. Several rubbery polymers or mixes were selected primarily based on research carried out in References [8]and [1]. Little data of the type needed on partition coefficients and diffusivities were found in the chemical literature searched. The polymers investigated are tabulated below:

TABLE 2: POLYMERS WHOSE PARTITION COEFFICIENT WAS MEASURED

Polymer	*Source*
DMS - Dimethyl Silicone	Dow Chemical
PECH - Polyepichlorhydrin	Aldrich Chemical Co.
Latex	Woodland Sconics, Lynn Creek, Mo.
PEM[a] - Polyethylene maleate	Dr. Arthur Snow, U.S. NRL
FPOL[b] - Fluoropolyol	Dr. Arthur Snow, U.S. NRL
ABACD[c] - Abietic Acid	Aldrich Chemical Co.
SEB -Styrene/ethylene-butylene	Aldrich Chemical Co.
(a) Mixture with DMS, 67% DMS - 33% PEM	
(b) Mixture with PECH, 50% FPOL - 50% PECH	
(c) Mixture with DMS, 50% DMS - 50% ABACD	

3.1 Feed Gas Generation

Feed concentrations were prepared by use of a bubbler system in which Nitrogen is saturated with gas vapor at a controlled temperature. The bubbler consists of a vessel two inches in diameter and twelve inches tall partially filled with glass marbles and the chemical liquid to be vaporized. Nitrogen gas is introduced at the bottom of the vessel and collected at the top. The saturated Nitrogen is then mixed with a second diluting stream to obtain the desired gas concentration and piped to the test apparatus. Concentrations were computed from equations for vapor pressure of DMMP and Toluene as follows:

$$p'_o(DMMP) = 10^{(11.102-3310/T_o)}, \tag{28}$$

and

$$p'_o(Toluene) = 10^{(8.323-2050/T_o)}, \tag{29}$$

where T_o is the gas/liquid equilibrium temperature in degrees Kelvin, and p'_o is the equilibrium vapor pressure in Torr. The DMMP relation was obtained from [5]. That for Toluene was obtained from [6]. Concentration exiting the bubbler is obtained from the ideal gas relation:

$$C = p'_o/RT_o, \tag{30}$$

where R is the gas constant for the particular gas.

Concentrations in the feed and exit of test modules are measured using two calibrated Gow-Mac model 12-800 flame ionization detectors (FIDs). FID calibrations are performed in two manners: by varying the amount of Nitrogen mixed with the DMMP feed from the bubbler and by varying the temperature of the water bath in which the bubbler is immersed. This latter method enables obtaining calibrations at the higher concentrations experienced during the elevated temperature of outbreath. Figure 17 presents calibration curves obtained by both methods that consist of FID output voltage versus equilibrium vapor pressure in torr. The calibrations are quite sensitive to the bubbler temperature as can be seen from equations 28 and 29. Good collapse of the calibration curves was found when corrected to a common temperature using the above equations. This also established the ability of the bubbler to achieve a saturated mix over a range of flow rates. The mixture flow rate to each FID is maintained constant and measured by a Cole-Parmer variable area flow meter. Feed flow rates to the FIDs for a given experiment were similarly controlled. The effect of feed flow rate on the calibrations is illustrated in Figure 17 for flow rates of 20 and 35 ml/min. The FID units were connected to a Gow-Mac 40-900 electrometer.

3.2 Property Measurement

Measurements of gas/polymer solubility and permeability were conducted in the experimental module depicted in Figure 18 over a range of temperatures. From these, values of the partition coefficient, K, and the gas diffusivity in the polymer were calculated as functions of temperature.

A thin membrane of the polymer whose properties were desired was mounted in a rectangular aluminum frame allowing an exposed polymer surface of 14.9 by 4.7 cm. The polymer membrane remained fixed to this frame throughout the experiments. The polymer/frame

assembly was sandwiched between two Plexiglas plates with a series of grooved channels cut in them to maintain good flow distribution over the membrane. The grooved channels were connected to small plenums machined in the Plexiglas at each end. The assembly was held together by clamping aluminum cover plates to the outside of the grooved Plexiglas plates. This arrangement enabled the module to be quickly disassembled to remove the polymer/frame assembly which was periodically weighed on a Mettler precision balance to determine the quantity of gas absorbed. A quick weighing was required to minimize any effects of mass exchange with the ambient air between the stopping point of the experiment and the actual weight measurement.

3.2.1 Permeability and Diffusivity

For permeability measurement the module configuration of Figure 18 is that of a counter flow mass exchanger with one gas stream entering port 1 and flowing down the membrane to exit at port 2 and the second gas stream entering at port 4, flowing counter to the first stream and exiting at port 3. The gas stream entering port 1 contains a known concentration of gas while that entering port 4 consists of pure Nitrogen. Thus the gas is absorbed by the membrane from the first stream, permeates across the membrane and is desorbed into the second stream. For steady flow with constant inlet conditions, such a system approaches a steady state equilibrium. For equal flow rates in each of the two streams and a constant thickness membrane, the steady state solution is readily provided by the counter flow heat or mass exchanger problem [7] and consists of a linear variation in concentration across the membrane and a concentration difference, ΔC, between the two channels that is independent of location along the channel:

$$C_1 - C_4 = C_2 - C_3 = \Delta C. \tag{31}$$

There is a diffusional resistance to mass flow from one side of the membrane to the other given by the sum of the resistances in the polymer membrane and in the two air channels (due to air boundary layers.) However, based on the geometry of the test setup and estimates of the boundary layer thickness from the mean groove height, the change in concentration across the air channels is less than 10% of that across the polymer membrane. Furthermore this resistance can be estimated from the channel dimensions and a correction made to reduce the uncertainty to less than a few percent. The value of ΔC is obtained using flame ionization detectors that measure the feed concentration, C_1, and the gas concentration, C_2, exiting port 2. Conservation of mass yields:

$$Q(C_1 - C_2) = Q(C_4 - C_3) = \Delta C K D_p A_M / \delta_p. \tag{32}$$

Here, Q is the volumetric flow rate, A_M is the Surface area of the polymer across which transfer occurs, and δ_p is the polymer membrane thickness. The term KD_p is related to the permeability via:

$$P = K D_p / RT. \tag{33}$$

3.2.2 Solubility and Partition Coefficient

For measurements of the solubility, referring again to Figure 18, feed concentrations are introduced at ports 1 and 3 and flow exiting port 2 and port 4 are fed to FIDs. Initially, the

concentrations of the streams exiting ports 2 and 4 are very low because of absorption by the membrane. When the polymer is saturated and equilibrium with the gas concentration is achieved, the concentrations of the exiting ports 2 and 4 are constant and equal to that of the input stream. Under these conditions, the solubility S is given by:

$$S = \frac{C_{eq}}{p'}, \tag{34}$$

where C_{eq} is the concentration of gas in the polymer at equilibrium with the gas phase at a partial pressure of p'. In terms of measurable quantities, this equation becomes:

$$S = \frac{\frac{\Delta m}{m_o}\rho_p}{f p'_o}\frac{p_o}{p}. \tag{35}$$

Here, Δm is the measured weight gain, m_o the initial polymer weight. Both were obtained using a precision Mettler H31 balance with a maximum range of 160 grams and a scale reading to one tenth of a milligram. ρ_p is the density of the polymer. The partial pressure of the gas. p'_0,is determined from its vapor pressure at the bubbler temperature. The dilution factor. f. is set by the flow meters and is the fraction of saturated concentration in the gas stream (e.g.. when the saturated flow out of the bubbler is mixed with an equal amount of pure Nitrogen. the resulting stream has a gas concentration 50% of the saturated value. and $f = 0.5$). The ratio of total pressure at the membrane, p, to total pressure at saturation conditions, p_o, is measured to be between 0.99 and 1.0 and is taken to be 1 for our experiments. Thus S is obtained from relation (34). The partition coefficient, K, is then obtained from the relation:

$$K = SRT. \tag{36}$$

For some cases where the solubility was low the accuracy of the measurements was unsatisfactory because the weight gain was too small for the Mettler balance. To overcome this problem another technique was employed to provide a much larger polymer sample weight and hence for a given solubility a larger weight gain. In this method the polymer samples were prepared by applying a thin film of polymer to a sheet of aluminum foil. The polymer was usually thinned by dissolving it in a solvent(Chloroform or Toluene). After driving off the solvent by heating in an oven at $150°C$, the foil sheet was folded to form a thin closed space about the polymer film. After preliminary weighing to obtain the polymer and foil weight a tube was inserted into the foil pocket and feed gas was fed at a rate of approximately one liter per minute. The lateral dimensions of the polymer on the foil were approximately 10 by 20 centimeters. To eliminate errors due to adsorption on the aluminum foil an uncoated dummy aluminum foil pocket of the same size was tested; however, the adsorption found was usually negligible. To obtain results at elevated temperatures the foil pocket was installed in an oven with controlled temperature.

3.3 Breathing Test Apparatus and Test Procedures

The simulated breathing test loop is shown schematically in Figure 19. It contains a bubbler system to provide feed at a preset concentration to an inbreath bellows pump that supplies the feed to the test module. On exiting the test module the majority of the flow is vented.

but a small fraction is fed to the flame ionization detector (FID #2) used to measure the exit concentration. The outbreath bellows sucks gas of controlled humidity and temperature back through the test module while six solenoid valves control the flows and are switched on or off to simulate breathing. The two bellows are driven by a motorized cam and provide for a sinusoidally varying flow through the test module. Before starting a test, the inbreath bellows and all piping leading to the test module are saturated with feed gas for one half an hour to assure full initial concentration to the test module. At the same time, the flow system to FID #2 is purged with pure Nitrogen to remove any adsorbed or absorbed gas. The system operates at atmospheric pressure by virtue of the vents provided. Flow pressure losses are small fractions of an inch of water; however, a pressure of about two inches of water is required to provide the flow through the FIDs. For FID#1 which measures the feed flow concentration this pressure is obtained by use of the throttle valve shown in Figure 19. A vacuum system provides flow to FID #2, and allows a constant flow of feed to the detector which is slaved to a strip chart recorder. The recorded data thus shows a time evolution of the gas concentration passing out of the test module. The bellows shown in Figure 19 are four inches tall and have an effective diameter of two and one half inches. Stroke volume was typically thirty milliliters and cycle periods were variable from five to eight seconds. All piping on the exit side of the module was insulated and heated to maintain flow temperatures.

3.4 Determination of Measurement System Time Lag

In the tests using the apparatus shown in Figure 19 adsorption on the tubing walls and in the flow meter could be a problem, and therefore it was important to measure the time lag in concentration between FID #2 and the test module exit. To provide a correct measure of this lag, a test was made to provide a step input of concentration at the module exit. This was done by operating the system in its oscillating mode by removing the module, connecting the module feed line directly to the module exit line and purging the lines to FID #2. A flow with known concentration was then introduced to the lines leading to FID #2, and the response was measured. Figure 20 shows the FID #2 response. Superposed on this figure is a best fit exponential approximation to the measured data. Using this approximation, analysis based on Laplace transforms provides a formula for correction of the concentration readings of FID #2 to correspond to the concentrations at the module exit. This relation incorporating the data of Figure 20 is:

$$\frac{C}{C_o} = \frac{C_{me}}{C_o} + t_c \frac{d(\frac{C_{me}}{C_o})}{dt}. \tag{37}$$

Here C is the corrected concentration, C_o is the feed concentration, C_{me} is the measured concentration at the FID, t is time in minutes and t_c is the characteristic time constant for the exponential response. t_c is found to be 1.4 minutes for our system, and the corrections required to our experimental data are found to be generally negligible.

3.5 Measurement Accuracy

Accuracy of the test results is influenced by many factors. Accuracy in measurement of concentration and gas flow rates is the most critical. The absolute level of the concentration is not a prime source of error because we are measuring the ratio of feed concentration to exit

concentration, and this ratio is expected to be independent of absolute concentration level. The measurement of the concentration by the FID is, however, subject to error caused by variation in hydrogen, air and carrier gas flow rates. Dirt and corrosion of the FID can also cause error in readings. However, zero checks at the beginning and end of each test run can identify any such shifts and were part of our procedures. The flow rates into the test module are imposed by the movement of the bellows in such a way that they are not influenced by feed flow meter errors. This is so because gas flows to the bellows are set at a value greater than that required by the bellows pump, and the excess is vented at ambient pressures. A similar arrangement is provided for the return flow volumes pumped by the bellows - i.e., the outbreath. The total volume pumped was measured over a number of cycles. Measured values are within one percent of those obtained from the product of effective bellows area and stroke. Other potential sources of error include possible leaks in the piping system and electrical interference in the electrometer output. The system was periodically checked for leaks by observing the ability of a section to hold a small vacuum or pressure. Electrical interference was observed in some tests as an oscillation in the FID outputs at cycle frequency. This effect was caused we believe by the impulses produced by switching on and off the solenoid valves.

The temperature variations that may occur during a long run or in repeating runs from one week to another may also introduce some errors. For example, a variation of one degree centigrade in the ambient room temperature may reduce the partition coefficient of the module by as much as 5%. This change is estimated to result in a comparable or smaller shift in the concentration measured. In all cases operating temperatures were monitored and recorded.

Consideration of the various sources of error leads to the conclusion that the data from the oscillating flow tests should be satisfactory for the engineering estimates of performance desired.

3.6 Polymer Test Modules

3.6.1 Modules Simulating Breathing

The test modules used for simulated breathing are described in the following listing:

TABLE 3: MODULES TESTED IN SIMULATED BREATHING EXPERIMENTS

Polymer	Gas		Module Tubes		Module Diameter (cm)
		Number	Radius (cm)	Length (cm)	
DMS	DMMP	139	0.079	1.27	2.54
"	"	139	0.079	2.54	2.54
"	"	414	0.025	1.27	2.54
Latex	DMMP	139	0.079	1.27	2.54
PECH	DMMP	foam	-	2.54	1.27
DMS	Toluene	414	0.025	1.27	2.54
"	"	414	0.025	5.08	2.54
ABACD/DMS	DMMP	particles	-	2.54	1.7
PECH	DMMP	280	0.018	3.8	1.27

For comparison with the analytical results modules of polymer were cast with many closely spaced holes. Of these two were made with 414 0.02 inch diameter parallel holes with lengths

of 0.5 and 2 inches. Two more were cast with 139 1/16 inch holes of 0.5 and 1 inch lengths. These modules were made by use of multiple rods of the desired diameter held in a drilled jig. The polymer was poured around the rods and allowed to polymerize in place after which the rods were withdrawn leaving the open holes. A schematic drawing of such a module is shown in Figure 21. Attempts to form a module from PECH in this way were not successful. The problem arises for this polymer because it has been liquefied by dissolving in Methylene Chloride. On evaporation of the solvent it was found that severe shrinkage and distortion had occurred and unacceptable voids were observed. Another technique was used for forming modules of polymers that required dissolution. The following steps were employed:

1. A flat membrane of about 10 mils in thickness was formed from a dilute solution of the polymer by evaporation. Several pourings were required to achieve the desired thickness.

2. A rack of rods 20 mils in diameter was made in the form of a ladder with a 30 mil spacing of the rods.

3. The ladder was pressed into the polymer membrane so that the rods penetrated the polymer to a depth of 5 mils. Shims were used to assure uniform penetration. The assembly was heated to $150°C$ to set the polymer before removing the rack. On completion the polymer membrane was flat on one side and corrugated on the other with a total thickness of 15 mils.

4. The membrane was then rolled around a 0.25 inch rod with the corrugations parallel to the axis of the rod.

5. Finally the rolled membrane and rod were potted in an aluminum casing prepared with end caps and entry and exit flow ports.

In an effort to provide a simple filter system modules were also prepared using an open polyurethane foam lattice in which PECH had been deposited. The open polyurethane foam used has a remarkable structure composed of many thin rod-like elements with relatively large open spaces between them. The specific gravity of the foam is as low as 0.02 or 0.03. If the rod like elements could be coated with a thin layer of absorbent polymer still maintaining most of the open area it would provide a good means for achieving rapid mass transfer from a permeating gas flow. To this end two modules of foam were made by passing a dilute solution of PECH through the foam and allowing it to dry. Test results were not encouraging for this method, and it was determined that the polymer had probably blocked the air passages rather than simply coating the structural elements of the foam.

A module was made of a mixture of Abietic acid and DMS by chopping it into stringy particles averaging 1/2 mm in diameter and 3 mm long and packing them loosely in a cylinder 17 mm in diameter and 25 mm long. The particles were held in place by fine screens at each end of the cylinder. The cylinder was provided with caps containing double ports for connection to the breathing apparatus. This polymer mix was not amenable to being cast in a parallel holed module.

3.6.2 Absorption Test Modules

To form membranes or for coating aluminum pockets described in section 3.2.2, polymers were first dissolved in a solvent such as Chloroform or Methylene Chloride and then the desired membrane was cast. The DMS membranes, however, were formed from a viscous liquid state after mixing with a curing agent. Membranes were cast by drawing a straight bar at a fixed height above a flat glass plate on which a sufficient amount of polymer had been spread. After polymerization in place the membrane was pealed from the plate and inserted in the exchanger of Figure 18.

4 Test Results

4.1 Partition Coefficient and Permeability Measurements

There are considerable data in the literature for partition coefficients and permeabilities for gases that are of commercial interest: O_2, N_2, CO_2, NH_3, etc. Data on organic vapors is sparse particularly for permeability. Reference [8] provides very useful data on partition coefficients for several polymers of interest and includes data for polymers versus various gases. Our data measured for PolyEpiChlorHydrin (PECH) and DMMP confirm the results of [2], and a mix of PECH and the compound Fluoropolyol shows the expected increases in partition coefficient due to that polymer as shown in the following.

Measured partition coefficients obtained are presented in Figure 22. As shown in this figure, polymers considered included DMS, PECH, Latex, Styrene/Ethylene-Butylene (SEB), a mixture of Fluoropolyol and DMS, a mixture of Fluoropolyol and PECH, a mixture of DMS and Polyethylene maleate (PEM) and a mixture of Abietic Acid and DMS. Gases were DMMP and Toluene. As anticipated by Raoult's law [9] the values for Toluene are much lower than those for DMMP although the inverse relation with vapor pressure is not found. Based on vapor pressure the extrapolation from DMMP to Toluene with DMS predicts a partition coefficient for Toluene of 400 whereas the measured value is roughly 1000. The data of Figure 22 are plotted versus concentration expressed as a percentage of saturation. Modest increases in K with decreasing concentration can be discerned for DMMP/DMS and DMMP/PECH + FPOL. The measured dependence of K on temperature is presented in Figure 23 for a range of temperature from 15-42° C. The values of K are seen to decrease with increasing temperature with the amount of decrease dependent on the polymer/gas pair. A factor of 2-3 is typical over this temperature range.

Measurements of the permeability of DMS and PECH to DMMP were made and are shown in Figure 24. The permeability of PECH is seen to be an order of magnitude lower than DMS and the computed diffusivity is two orders of magnitude lower. DMS at room temperature has a value of diffusivity of $2{\cdot}10^{-7}$ cm^2/sec in agreement with the results of Reference [1]. PECH is computed from the data to have a diffusivity of $10^{-9} cm^2/\sec$, surprisingly low for a rubbery polymer. These measurements established the bounds for these parameters in the analytical computations.

4.2 Simulated Breathing Tests

A series of simulated breathing tests were conducted in the simulated breathing loop described previously. A summary of the test modules employed has been previously presented in Table 3. The modules listed provide for a variation in tube length and diameter. In addition to these geometric and property variations, the velocity through the tubes and breathing rate were varied. Such data are critical to determining design trade-offs such as length versus number of tubes. The data obtained have been compared with results of numerical simulations and are discussed below.

We began our experimental program with DMS modules and DMMP as the gas contaminant, and these results are discussed first. Figure 25 presents results of three repeated runs conducted over a period of hours for DMS and DMMP with the 414 tube 1.27 cm long module (R_a =0.025 cm) at a base breathing rate of 10/min. Data is presented as the ratio of the concentration measured at the mouth C_m to the input concentration, C_o, which was typically set at 15% of the saturated value. The simulated breathing was conducted continuously until the measured concentration at the mouth (x=L) stopped showing any significant variations and thus attained a constant saturated value - in this case at 8 hours a value of approximately 10% of C_o. The three curves provide a measure of repeatability of the experiment for this configuration. At 2 hours of breathing, the variation is about 30% about the mean value while at 8 hours, the variation is about ± 5% about the mean. Also shown on figure 25 are the results of two numerical simulations of this case denoted by the solid and dashed lines. These were run for K=11,700, our best estimate of K from our measurements (see Figures 22 and 23) and for two values of the polymer diffusivity, D_p. The lower value is our best estimate based on measured values. However, due to potential uncertainty in the data, we also selected a larger value of D_p which should represent an upper bound on the value. Both simulations are seen to compare well with the overall levels of the experimental data. The higher diffusivity calculation is seen to be a better short term match to the data while the lower diffusivity case is seen to better predict the longer term performance. Of significance is the fact that the experimentally measured concentrations at the mouth are lower than those predicted by the model resulting in better respirator performance than that predicted by the model. This is a general trend that we have observed in comparing experimental and numerical results. The difference is generally most pronounced at short times. We believe this may be due to concentration dependent properties at very low concentrations not included in the numerical model. This is discussed more fully below.

4.2.1 Influence of Velocity

Figure 26 presents the measured influence of the velocity in the module tubes by comparing one of the curves of Figure 25 run at a velocity of 12.2 cm/s with a case run under identical conditions except at a mean velocity of 6.1 cm/s. The effect is seen to be substantial with the lower velocity case resulting in a measured concentration ratio of only 0.3% after 10 hours compared to over 9% for the higher velocity case. *This is a 30 fold improvement for a reduction in the velocity by a factor of two.* In addition, the lower velocity run has not achieved saturation after 12 hours while the higher velocity case saturates at about 8 hours. We have found such large influences on the pre-saturation performance due to velocity (and

other parameters as seen below) throughout our work. The asymptotic analysis for prediction of the saturated performance presented in section 2.5 suggests that saturated performance varies simply as the inverse of velocity. What is of great importance to respirator design is that performance in shorter times typical of respirator operation - a few hours - is much more sensitive to such parameter changes.

4.2.2 Influence of Breathing Rate

Figure 27 presents the measured effect of breathing rate. In this case, the same total volume of air per breath was maintained, but the rate was varied from the base case of 10 breaths/min to higher rates of 12 and 15 breaths/min indicative of the effects of exertion. Thus, experimentally, both the cycle period was shortened and the mean velocity increased to maintain the breath volume. In our experimental setup, this is accomplished by increasing the rotation rate of the cam driving the bellows. As expected, the higher breathing rates produce higher concentrations at the mouth. The nonlinear nature of performance prior to saturation is again evident. For example, breathing rates of 12 and 15 per minute represent increases in cycle mean velocity of 20% and 50%, respectively (and proportional decreases in period). At 4 hours of breathing, measured exit concentrations have increased by approximately 20% and 85%, respectively.

4.2.3 Influence of Module Length

The effect of module tube length is shown in Figure 28. Here, data from DMS modules of tube radius 0.079 cm and lengths of both 1.27 and 2.54 cm are presented for DMMP and a velocity of 3.7 cm/s. Data from two runs with the longer module are presented and are seen to exhibit very good repeatability. The nonlinear nature of the response with tube length is apparent. At 4 hours of breathing, the shorter module produces a concentration of 10% of C_o. However, doubling the module length cuts the measured concentration at 4 hours to 0.4% of C_o - a factor of 25 reduction in measured concentration. Also shown in this figure are the results of numerical simulations of the two cases. Comparison of predicted and measured performance for the shorter module is seen to be quite good. However, the model is seen to significantly under predict performance for short times for the long module. We believe this may be due to concentration dependent effects in which the value of the partition coefficient increases at very low concentrations. Such behavior is often observed in both absorption and adsorption phenomena.

4.2.4 Dependence of Properties on Concentration

To check the plausibility of the explanation above, a simple nonlinear variation of the partition coefficient K was assumed and utilized in the numerical model:

$$K = \frac{K_o}{(\frac{K_o}{K^*} - 1)(\frac{C}{C^*}) + 1}, \; C \leq C^*, \tag{38}$$

$$K = K^*, \; C \geq C^*. \tag{39}$$

In this relation, the value of K is independent of the concentration and equal to K^* for values of the concentration larger than C^* and rises smoothly with decreasing concentration to K_o, the value at zero concentration. The results of these calculations are presented in Figure 29 Here the value of C^* was taken to be equal to the minimum value at which K was obtained experimentally (10% of saturation) which corresponds to 0.65 C_o in the experiments. Two cases are presented, for $K_o/K^* = 2$ and 5 with K^*=11,700, together with the calculation for constant K and the experimental data of Figure 28 for the 1.27 cm long module. The assumed variation of K with C is presented in Figure 30. As can be seen, the use of this concentration dependent partition coefficient results in predictions that more closely agree with experimental data at short times. Since the selection of the variation of K was arbitrary, one might expect closer correspondence with a better expression of the actual variation of K with C which was not measured.

4.2.5 Polyurethane Foam Modules

Results of tests made using polyurethane foam coated with PECH (described in Section 3.41) are shown in Figure 31. It can be seen that the module with a heavier coating of PECH gave poorer results than the one with a lighter coating. This is probably due to an improper method of coating the foam which resulted in the polymer blocking the air channels causing increased flow velocities.

4.2.6 PECH Rolled Module Test

The PECH module described in Section 3.6.1 was tested using DMMP as the feed gas and the results are presented in Figure 32. The rapid rise of concentration was disappointing for this module as PECH was found to have a large partition coefficient and would be expected to have a performance better than any of the other polymers tested. To determine the cause of the poor performance the module was cut open and it was found that the channels were severely blocked. Further attempts to produce a PECH module failed. It was concluded that direct foaming of the polymer or perhaps casting with polymerization in place could succeed. However, these methods would require a significant development effort and were not pursued.

4.2.7 Tests with Toluene

Figure 33 presents results of simulated breathing tests with toluene for two different DMS modules with a value of R_a= 0.025 cm. In the first case, the same module and conditions are employed as used for DMMP in Figure 25 (L = 1.27 cm, U_{mean}=12.2 cm/s). As can be seen in this figure, the measured concentration at the mouth rapidly saturates to a value of 20% of C_o after approximately 45 min. The second case (L = 5.08 cm, U_{mean} = 6.1 cm/s), as expected from discussions in the previous sections, produces substantially lower exit concentrations. After 2 hours of breathing, the exit concentration is only 0.1% of C_o (versus 20% for the first case) and at 3.2 hours, it is still only 0.3% of C_o compared with the saturated value of 20% for the first case. Also shown on this figure are the results of several numerical simulations. Since the experimentally observed performance was much better than that predicted numerically with the measured value of K=1000, a higher value of K=2000 was tried. As can be seen in this figure, use of K = 2000 provides a better match but still over predicts the results

4.3 Importance of Two-Way Flow

Figure 34 presents a comparison of performance of the two-way flow concept for the conditions of Figure 25 with that of the conventional "one-way" flow configuration typical of a conventional respirator design in which a separate outbreath valve is employed. In order to simulate this experimentally, the "outbreath" flow was disconnected from the module. Thus the module experienced an inbreath followed by a pause with no flow through it followed by the next inbreath. This figure provides a graphic illustration of the advantage of the two-way breathing approach. After two hours, the measured concentration is 80% of C_o for one-way breathing, but only 2.5% for the two-way mode.

5 Respirator Design Considerations

The goal of the research presented here is to develop respirators that are lighter and more compact than those presently available that use activated charcoal as the filter medium. The concept envisioned a porous absorbent polymer material formed in the manner of a surgical mask through which breath is both inhaled and exhaled. The absorbent polymer would constitute the major weight of the respirator. Its value can be expressed by the relation

$$PolymerWeight = \rho_p LA(1-\varepsilon),$$

where ρ_p is the polymer density, L the polymer thickness (channel length), A the total face area of the filter and ε is the fraction of A occupied by the channel holes. For holes spaced at the corners of equilateral triangles making use of Equations (1) and (2)

$$\varepsilon = \frac{\pi}{2\sqrt{3}}(\frac{R_a}{z})^2 = (\frac{R_a}{R_p})^2. \tag{40}$$

For a given mean respiration volumetric flow rate, Q, (typically 30 to 40 liters per minute) the face area, A, and the mean apparent flow velocity U_A are related by

$$Q = U_A A, \tag{41}$$

and in terms of the channel velocity,

$$U_{mean} = U_A/\varepsilon. \tag{42}$$

Combining the above relations we get for the polymer weight:

$$Polymer\ Weight = \rho_p QL(\frac{R_p^2}{R_a^2} - 1)/U_{mean} = \rho_p QL(1 - \frac{R_a^2}{R_p^2})/U_A. \tag{43}$$

For a desired performance specified by the breakthrough time to reach a limiting exit concentration of toxic gas, the analyses and tests described above show the desirability of low mean velocity and long channel lengths whereas low weight as seen from Equation 43 requires just the opposite. In the design of a respirator this clearly constitutes a trade-off problem. The selection of L and U_A must be made to ensure an adequate performance in removing

toxic gases from the entering air. The performance of the filter is also dependent on the polymer gas properties, partition coefficient and diffusivity, as well as the channel hole radius and spacing. If a specific toxic gas is targeted it may be possible to find a polymer having very good absorption characteristics. An example of this being the polymer Fluoropolyol and DMMP; however, for other toxic gases Fluoropolyol has rather poor absorptive capability and would not be suitable for general use.

5.1 Breathing Resistance

The favorable effect of small channel dimensions is limited by the requirements of low breathing resistance. For the channels of interest in respirators, the Reynolds numbers of the flows are so small (less than 10) that fully developed laminar flow is to be expected. The pressure loss in breathing can therefore be expressed by the following relation:

$$\Delta p = 8\mu U_{mean} L/R_a^2, \tag{44}$$

in which μ is the viscosity of the air. For values of U_{mean} as high as 24 cm/sec, radii of .0254 cm and channel lengths of 5 cm, a pressure loss of approximately 3 mm of water is predicted. Somewhat higher pressure loss can easily be sustained and would allow reductions in channel diameters with their favorable effect on performance. The Mine Safety and Health Administration suggests pressure losses at 85 liters/minute of 60 mm of water as being reasonable for pesticide respirators. For this level of loss the tube radius in the cited example could be reduced from 0.0254 cm to 0.0057 cm.

5.2 Ambient Atmosphere Concentration Effects

In order to design a respirator for use in toxic environments the levels of concentrations of the toxic gases must be specified. Thus NIOSH approves respirators for use under specific conditions such as a liquid spill in a room where nearly saturated conditions may prevail or for more usual cases where only a fraction of saturation occurs. For example, NIOSH approval for cartridges filtering Carbon tetrachloride vapors requires a maximum concentration at breakthrough of 5 ppm when breathing in an atmosphere of 5000 ppm. This is a value of C_m/ C_o equal to 0.001, but other values higher or lower will be of interest for other toxic gases and other ambient workplace conditions. The 5000 ppm value is only 12% of saturated vapor concentration at $25°C$ and the performance in terms of C_m/C_o of a respirator for more fully saturated conditions would have to be correspondingly better. Thus it is clear that the size and weight of the respirator will depend on the conditions imposed. For the present oscillating system using polymers as absorbers, the performance of the system measured by the ratio of intake to breathed toxic gas concentrations tends to be independent of concentration levels. This is true because the partition coefficients of the polymer/gas combination are generally independent of concentration[8] except possibly at very low concentrations. For activated charcoal however, the performance tends to be dependent on the feed concentration because the adsorbtion isotherms show a remarkably higher rate of adsorption at low concentrations than at high concentrations. To illustrate the differences discussed between oscillating respirator systems and activated charcoal systems we have considered the potential sizes and weights

for two cases, one for a toxic gas like DMMP and another for Toluene. The assumptions for DMMP are:

Allowable TLV (Breakthrough)	16 ppb
Allowable Maximum Concentration	132 ppm
Saturated Concentration	1320 ppm
Duration to Breakthrough	4 hours
Polymer/Gas Partition Coefficient	40,000
Polymer/Gas Diffusivity	$2x10^{-7}$ cm^2/s
Mean Inspiration Air Flow(inbreath)	30 liters/min
Hole Radius	0.0127 cm

The resulting system size and weight are:

Frontal Area	120 cm^2
Polymer Thickness	1.3 cm
Polymer Weight	85 gms
Carbon Weight[2]	4 gms

The computations above are based on a measured value of 40,000 for the partition coefficient for a polymer mix of DMS and Abietic acid and a value for C_m/C_o of 0.00012. These predictions have not been directly verified by module tests: however, tests of DMS alone have shown the computations to be conservative and to underestimate the performance. The assumptions for Toluene are:

Allowable TLV	100 ppm
Allowable Maximum Concentration	12,500 ppm
Saturated Concentration	36,800 ppm
Duration to Breakthrough	4 hours
Polymer/Gas Partition Coefficient	2000
Polymer/Gas Diffusivity	$2x10^{-7}cm^2/s$
Mean Inspiration Air Flow(inbreath)	30 liters/min
Hole Radius	.0254 cm

The resulting size and weight are:

Frontal Area	236 cm^2
Thickness	5.1 cm
Polymer Weight	768 gms
Carbon Weight[2]	580 gms

Experimental measurements and numerical estimates for a polymer absorbing Toluene were presented in Figure 33. The design point selected is a value of C_m/C_o equal to 0.008 at 4 hours. The assumed value of 2000 for partition coefficient used in the estimate above is based on the assumption that a modest increase over the values measured can be obtained with a suitable mix such as DMS/Abietic acid or DMS/FPOL. A decrease in the channel radii would

[2]Does not include weight of canisters and supporting structure required for granualted carbon estimated to be at least 150 grams.

also increase performance and an extrapolation of the experimental values to 4 hours also validates the assumptions made for this calculation. We therefore believe this estimate to be conservative. Note that the maximum allowable environmental concentration shown for the first case is 10 % of the saturation value and corresponds to a concentration of 67 $\mu gm/liter$. In the second example the environmental concentration of 12,500 ppm is 34% of saturated concentration at $25°C$, (37,800 ppm) corresponding to a concentration of 480 $\mu gm/liter$.

5.3 Comparison with Activated Charcoal

Estimates of the charcoal weight required for the two cases discussed above were made using data for DMMP from [10] and data obtained for Toluene from [11]. A simple bed of activated charcoal was assumed with a working factor of 66%. This implies a 66% saturated bed at breakthrough. This simplified approach was considered adequate for the engineering comparisons being made. The weight of carbon computed for the DMMP case was 4 grams as compared to the 85 grams estimated for the polymer with oscillating flow but additional weight must be assigned to the carbon beds for supporting face masks and cannisters. A typical value for this weight would be 150 grams. The polymer can be considered to be able to support its own weight. It appears from this example that the two way flow system is competitive in weight with conventional charcoal respirator systems for gases having partition coefficients with the polymer of 40,000 or more and may offer the possibility for more compactness and ease of wearing. For the Toluene case a carbon weight of 580 grams was obtained to be compared with the 768 grams estimated for the polymer. Again the added weight for cannisters etc. make the two systems on a par from the weight standpoint. The large weight for the charcoal bed is the result of the high feed concentration. The charcoal weights were calculated from a simple mass balance,

$$C_o Q \cdot (Break\ through\ time) = (Carbon\ capacity \cdot Working\ factor), \qquad (45)$$

where Q is the breathing rate and Carbon capacity is the weight of gas adsorbed in the carbon per unit weight of carbon. Obviously the Toluene filters, both activated charcoal and two way flow, considered here are large and heavy for use in a workplace. Nevertheless for such an extreme environmental concentration of toxic gas (34% saturated) an alternative supplied air system would weigh considerably more.

The above considerations were made for protection against vapors at high environmental saturation percentages. At low environmental concentrations of the gases considered, DMMP and Toluene, the required values of C_m/C_o are higher because the TLV values will of course be the same. In the DMMP example the C_m/C_o ratio was 0.00012 for ambient air at 10% saturation For ambient air at 1% saturation it would be 0.0012 and the two way polymer system could be reduced in weight and size but not in the proportion to the saturation ratios. The calculated carbon weight would simply be reduced by the saturation ratios as seen referring to Equation 45. In this case the carbon weight is negligible. For Toluene, and an ambient concentration maximum of 1% of saturated a modest reduction in weight of the polymer can be expected whereas the carbon weight required is reduced by a factor of 34 to 17 grams. and a commercial respirator approved for organic vapors would suffice. We conclude that for near saturated ambient conditions the polymer based system can compete with the

activated charcoal respirator systems but both systems become heavy as the vapor pressure of the toxic gas increases. More will be said about this effect in Section 5.4 below. At low saturated conditions the polymer system can still offer reasonable and competitive weights but rapidly becomes heavier as the vapor pressures of the toxic gases increase.

A comparison of the adsorptive or absorptive isotherms for polymers and activated charcoal provides insight into the differences between the two. Figure 35 presents isotherms for activated charcoal and polymers versus DMMP. One advantage of activated charcoal in one way flow over polymer absorbers is seen by the large differences in capacity over the low concentration range. Only Fluoropolyol which has an extraordinary affinity for DMMP appears competitive on this particular point. Even here Fluoropolyol could not absorb DMMP to the large fraction of its own weight shown without substantial swelling. Beyond an absorption ratio of 0.2 or so the extension of the linear curve is therefore dashed as questionable. The favorable (convex upward) isotherm exhibited by the adsorptive systems also conveys an advantage because at breakthrough the adsorbant bed can approach a more fully saturated condition.

The advantage of the polymers, however, lies in their ability to be utilized in two way flow with the outbreath desorbing and expelling much of the toxic gas absorbed on the inbreath.

5.4 Absorption of High Vapor Pressure Compounds

For protection against low boiling point vapors such as Methylene Chloride or Vinyl Chloride the polymers used to date do not provide sufficient absorption to be useful in a workplace respirator system. This conclusion is illustrated by the performance predictions shown in Figure 36. Here the partition coefficient of 25 is estimated as reasonable using an extrapolation of Raoult's law for Methylene Chloride and DMS. The system is seen to reach equilibrium very quickly (a few minutes) and to attain an equilibrium reduction in concentration of only 37%. Using an optimistic value for partition coefficient of 100 and a lower channel velocity improves the system but the concentration reduction is still too little (82%) and the filter weight would exceed an unrealistic 3.6 pounds. Activated charcoal systems also become heavy for these gases and generally supplied air systems are to be preferred.

5.5 Respirator with Supplemental Air

In oscillatory breathing the return air acts to scavenge the absorbant material of toxic gases and it would appear that an increased backflow at some value could completely prevent the entrance of toxic gas to the breather. If this were possible a system using much less supplied air could be built. For example, if the back flow was twenty percent of the air required for breathing, a tank of air would last five times as long as when breathing directly from the tank without the absorbant mask. To investigate this possibility computational runs were made and several experimental tests were performed. The analytical results are shown in Figure 37 for several values of the ratio of supplied air to breathing air. It can be seen that a marked reduction in the exiting air concentration is obtained; however, even though at 32% supplemental air the oscillating flow system does not reject all the entering toxic gas the concept appears worthy of further more detailed study. An experimental simulated breathing test using 9.4 % supplemental air was performed and the results are presented in Figure 38.

These tests were made with the Abietic Acid/DMS particle module described earlier. Again the data show the favorable effect predicted.

6 Conclusions

Breathing forward and backward through polymer lined channels has been studied both analytically and experimentally and the following general conclusions have been reached:

1. Relative to direct one way flow through the channels there is an order of magnitude increase in the time to reach any specified exiting concentration.

2. The oscillating flow system is found to reach a final equilibrium value of the exiting concentration at a fraction of the entering concentration. This is not possible with a one way flow system.

3. The temperature distribution in the polymer was found in computations to be linear from entrance to the mouth exit varying from ambient atmospheric temperature to body temperature.

4. Polymer gas pair partition coefficients and diffusivities have been shown to be of primary importance in maximizing breakthrough time to a limiting concentration.

5. Performance of the channeled polymer filters was nonlinear with regard to increases in length or decreases in apparent velocity, particularly at times well before reaching an equilibrium. Halving the apparent velocity or doubling the length was found to result in an order of magnitude decrease in concentration at the mouth.

6. Numerical simulations were shown to predict the trends and approximate performance of experimental data. However, experiments were found to consistently produce lower concentrations than those predicted particularly at short times.

7. The concept of using two-way breathing through a polymer respirator in conjunction with a supplemental air supply was shown to be able to extend the life of the air supply by factors of three or more by exhaling the additional supplemental air back through the respirator.

8. Two-way breathing using polymeric absorption was found to be competitive with activated charcoal for ambient conditions with gases at high percentages of saturation. Both systems become heavy, and bulky, however, as the vapor pressures of the toxic gases to be removed increase. At low saturation ambient conditions both systems grow in weight with increasing vapor pressure of the toxic gases but two-way breathing systems with polymers examined in this study rapidly grow too heavy for practical use in the workplace.

References

[1] Hagel, D., Laverty, V., and Brown, C., "A Basic Research Study of Factors Affecting the Collection Efficiency and Power Use of High Volume Sampling Systems," *Hydronautics, Inc. Tech. Rpt. 7413-1*, May 1977.

[2] Peyret, R. and Taylor, T., "Computational Methods for Fluid Flow," *Springer-Verlag, New York*,1983.

[3] Brown, C., Kalumuck. K., Chahine, G., and Frederick, G., "Lighter Compact Respirators for Toxic Vapor Protection," DYNAFLOW, INC. *Tech. Rpt. 92003-1 (NIOSH Phase I SBIR)*, June 1993.

[4] "Threshold Limit Values and Biological Exposure Indices for 1989-1990," *American Conference of Governmental Hygienists, Cincinati, OH.*

[5] Personal Communication with Leon Schiff, Edgewood Arsenal, Aberdeen, MD.

[6] Perry and Green, Chemical Engineers Handbook,McGraw-Hill, New York.1984.

[7] Rohsenow, W. and Choi, H., *Heat, Mass, and Momentum Transfer*, Prentice-Hall, Englewood Cliffs. NJ, 1961.

[8] Grate, J., Snow, A., Ballantine, D., Wohltjen, H., Abraham, M., McGill, R. and Sasson. P., "Determination of Partition Coefficients from Surface Acoustic Wave Vapor Sensor Responses and Correlation with Gas-Liquid Chromatographic Partition Coefficients." *Anal. Chem, 60 869-875*, 1988.

[9] Wark, K., *Thermodynamics*, McGraw-Hill, New York, 1971

[10] *Tollen, E. D., "Sorption Properties of Activated Carbon," Comprehensive rt - Contract DA18-035-AMC-10953(A), Edgewood Arsenal, MD*, 1968.

[11] Yaws,C.L, Li,Bu, Nijhawan,Sachin. "*Adsorption-Capacity Data for 283 Organic Compounds*" Environmental Engineering World,May-June 1995.

[12] White, F.M., "Viscous Fluid Flow," McGraw Hill, New York, 1974.

7 Appendix

7.1 Analysis of the Equilibrium State

At equilibrium the variation of concentration along the channel is assumed to be linearly falling from the entrance to the exit. We consider the case of uniform temperature and constant properties for the polymer. The timewise variation due to breathing is taken as sinusoidal with a period of 2τ. The velocity distribution is assumed to be laminar and fully developed. It is expressed as

$$U(r,t) = \pi \cdot U_{mean}(1 - \frac{r^2}{R^2}) \cdot \cos\frac{\pi t}{\tau}. \tag{46}$$

The concentration of toxic gas in the channel is written as the superposition of two components, one, C_x, only a function of x ,the other C_o, a function of the radial distance and time.

$$C(x,r,t) = C_x(x) + C_a(r,t), \tag{47}$$

that is, all stations along the axis have the same variation in the radial direction and time. The differential equation governing the mass transfer in the air channel is from Equation (18)

$$\frac{\partial C}{\partial t} = \frac{D_a}{r}\left[\frac{\partial}{\partial r}(r\frac{\partial C}{\partial r}) - U\cdot\frac{dC_x}{dx}\right]. \tag{48}$$

It can be shown that for the cases of interest having high absorption of the toxic gases the storage of the contaminant in the carrier gas is very small relative to that in the polymer and the term on the left hand side of the equation can be neglected relative to those on the right. That is, at any point in the channel the variation of concentration in time is small whereas the terms on the right hand side are large and thus the left hand term is set to zero. It is then possible to solve the equation above for the radial concentration distribution. After a double integration with respect to r and making use of Equation (46) and the boundary condition of zero slope at the centerline,we obtain:

$$C = C_x + C_w(t) + (\frac{\pi}{4D_a}U_{mean}R_a^2\frac{dC_x}{dx})\cos\left(\frac{\pi t}{\tau}\right)(3/4 - \frac{r^2}{R^2} + \frac{r^4}{4R^4}), \tag{49}$$

where C_w is the wall value of C_a.

For thin polymer tubes, axial diffusion in the polymer can be neglected relative to that radially and the differential equation to be satisfied is (48) without the convection term on the right. The solution for sinusoidal oscillations is well known, Reference [12]:

$$C_{p=}KC_{wa}\exp(-\sqrt{\frac{\pi}{2D_p\tau}}y)\cos[(\frac{\pi t}{\tau} - \lambda) - \sqrt{\frac{\pi}{2D_p\tau}}y]. \tag{50}$$

Here C_{wa} is the amplitude of the wall concentration oscillations, and we have used the equilibrium condition at the wall, $KC_w = C_{pw}$. λ is the phase angle between the wall concentration and the velocity oscillations. From Equation (48) we now compute the radial mass flux per unit area at the wall.

$$-D_p\frac{\partial C_p}{\partial r} = KC_{wa}\sqrt{\frac{\pi D_p}{2\tau}}[\cos(\frac{\pi t}{\tau} - \lambda) - \sin(\frac{\pi t}{\tau} - \lambda)], \qquad (\mathrm{r}=\mathrm{R}_a). \tag{51}$$

Note that the term in the brackets can be rewritten

$$\sqrt{2}\cos(\frac{\pi t}{\tau} - \lambda + \frac{\pi}{2}). \tag{52}$$

The flux into the polymer must be supplied by diffusion from the air channel:

$$D_a\frac{\partial C_a}{\partial r} = (\frac{\pi}{4}U_{mean}R_a\frac{dC_x}{dx})\cos\frac{\pi t}{\tau}, \qquad (\mathrm{r}=\mathrm{R}_a). \tag{53}$$

As these fluxes must be in phase we obtain on equating the relations of Equations (51) and (53):

$$\lambda = \frac{\pi}{4}, \tag{54}$$

and

$$C_{wa} = \frac{1}{4K}\sqrt{\frac{\pi\tau}{D_p}}U_{mean}R_a\frac{dC_x}{dx}. \tag{55}$$

Equation (46) can now be written as:

$$\begin{aligned} C(x,r,t) &= C_x + C_{wa}\cos(\frac{\pi\tau}{\tau} - \frac{\pi}{4}) + \frac{\pi}{4}\frac{U_{mean}R_a^2}{D_a}\frac{dC_x}{dx}\cdot \\ &\quad \cos\left(\frac{\pi t}{\tau}\right)\left(\frac{3}{4} - \frac{r^2}{R_a^2} + \frac{r^4}{4R_a^4}\right). \end{aligned} \tag{56}$$

The phasing of the flow velocity and concentration oscillations in the channel results in a net flux of contaminant gas along the channel. This flux can be expressed as

$$\frac{Flux}{Cycle} = 2\pi\int_0^{2\tau}\int_0^{R_a} C(x,r,t)U(r,t)r\,dr\,dt. \tag{57}$$

There is in addition a flux due to simple diffusion along the mean concentration gradient dC_x/dx, that is:

$$\text{Axial Diffusional Flux per Cycle} = 2\pi\tau D_a R_a^2\frac{dC_x}{dx}. \tag{58}$$

The sum of these two fluxes divided by the inflow, $\pi\tau R_a^2 U_{mean}$, for one half a cycle will equal the mean concentration exiting the channel, C_m:

$$\begin{aligned} C_m &= \frac{2\pi}{\tau}\frac{C_{wa}}{R_a^2}\int_0^{2\tau}\int_0^{R_a}\{[(1-\frac{r^2}{R^2})\cos(\frac{\pi t}{\tau} - \frac{\pi}{4})\cos\frac{\pi t}{\tau}] + \\ &\quad [\frac{\pi^2 U_{mean}}{2\tau D_a}\frac{dC_x}{dx}(1-\frac{r^2}{R^2})(\frac{3}{4} - \frac{r^2}{R_a^2} + \frac{r^4}{4R_a^4})\cos^2\frac{\pi t}{\tau}]\}r\,dr\,dt. \end{aligned} \tag{59}$$

Introducing the expression for C_{wa} (equation 55), the axial flux terms and performing the integrations we obtain for the exiting concentration

$$C_m = [\frac{1}{2K}\sqrt{\frac{\pi\tau}{D_p}} + \frac{0.719\cdot R_a}{D_a} + \frac{8\cdot D_a}{R_a U_{mean}^2}]\frac{R_a U_{mean}}{4}\frac{dC_x}{dx}. \tag{60}$$

The axial concentration gradient will be reduced by the finite values of C_m at the exit as well as by the mean reduction of C_o at the entrance. We therefore write for the gradient

$$\frac{dC_x}{dx} = \frac{C_0 - 2C_m}{L}. \tag{61}$$

Solving Equations (57) and (58) for $\frac{C_m}{C_0}$ we finally obtain

$$\frac{C_m}{C_0} = \frac{N}{1-2N}, \tag{62}$$

where

$$N = [\frac{1}{2K}\sqrt{\frac{\pi\tau}{D_p}} + \frac{0.719\cdot R_a}{D_a} + \frac{8\cdot D_a}{\pi R_a U_{mean}^2}]\frac{\pi R_a U_{mean}}{4L}.$$

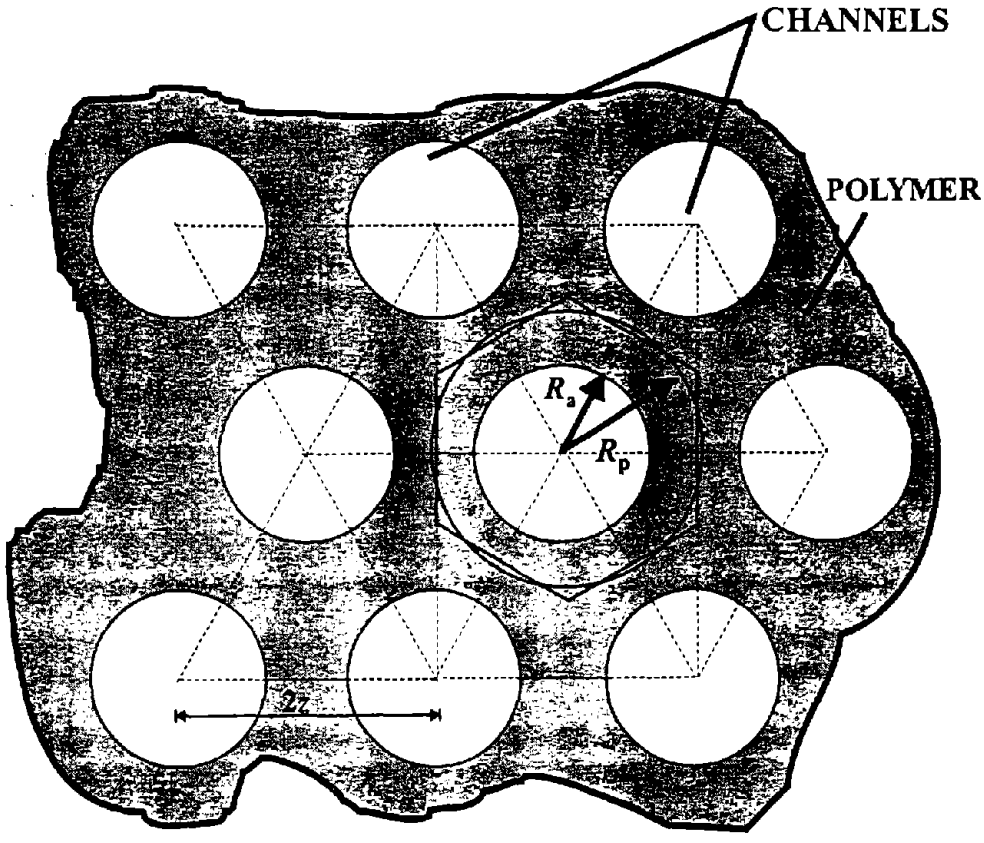

Figure 1: Sketch of an Idealized Respirator with Parallel Cylindrical Holes.

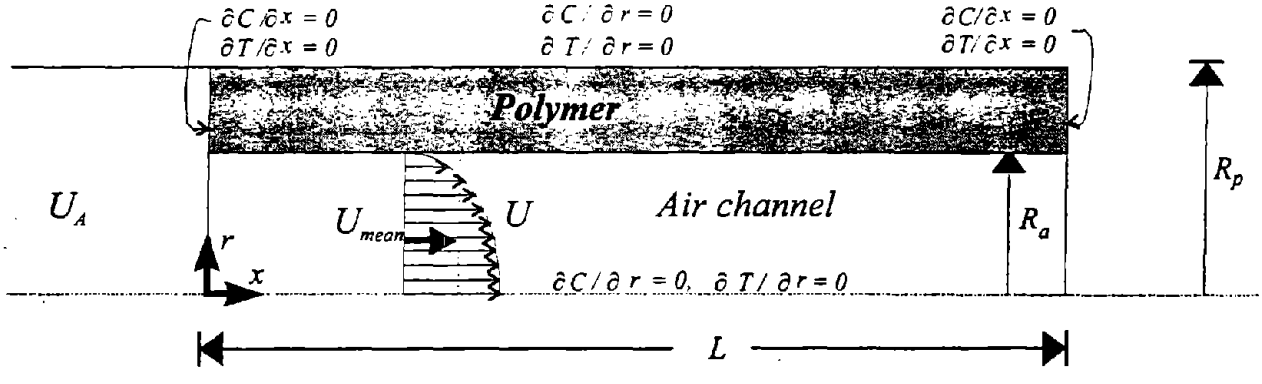

Figure 2: Sketch of Computational Model Domain.

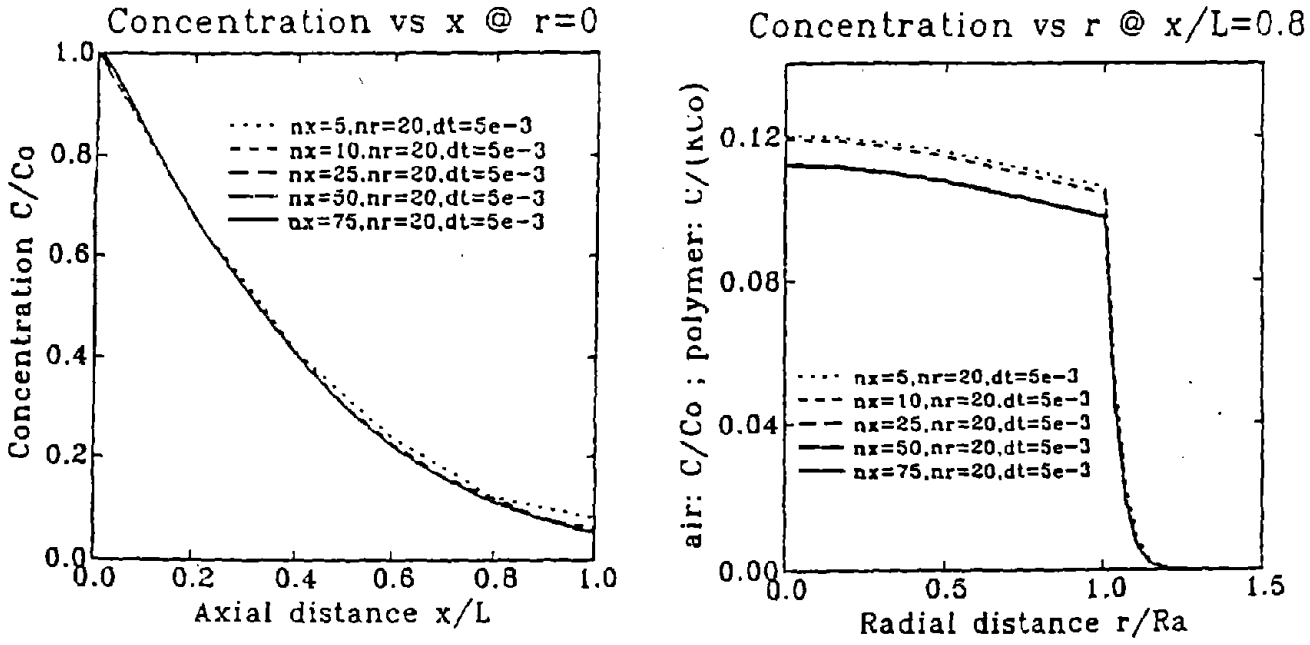

a: Computation with Varying Number of Axial Nodes and 20 Radial Nodes. Time Step Kept Constant.

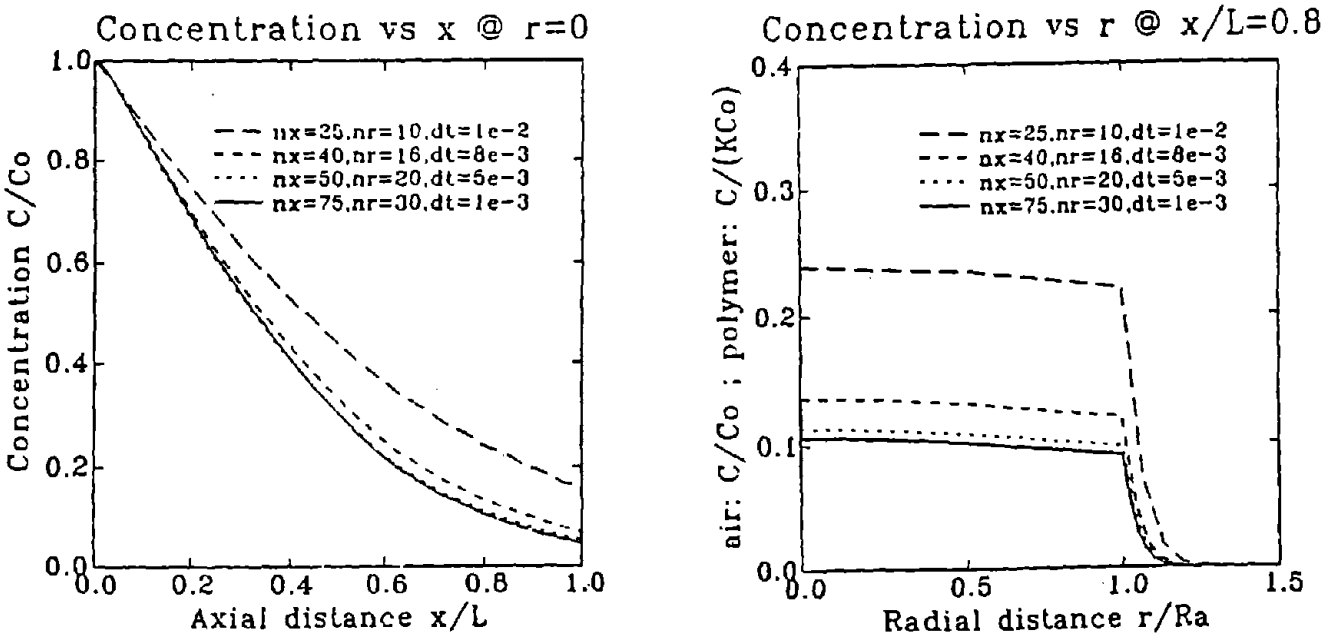

b: Computation with Fixed Ratio of Axial to Radial Nodes and Maximized Allowable Time Step.

End of 1st Half Cycle

$T = 240$ sec $K = 7500$ $U_{mean} = 10$ cm/s

$D_A = .075$ $L = 12.7$ cm

$D_p = 2 \times 10^{-7}$ $R_s = .08$ cm

Figure 3: Results of Convergence Study.

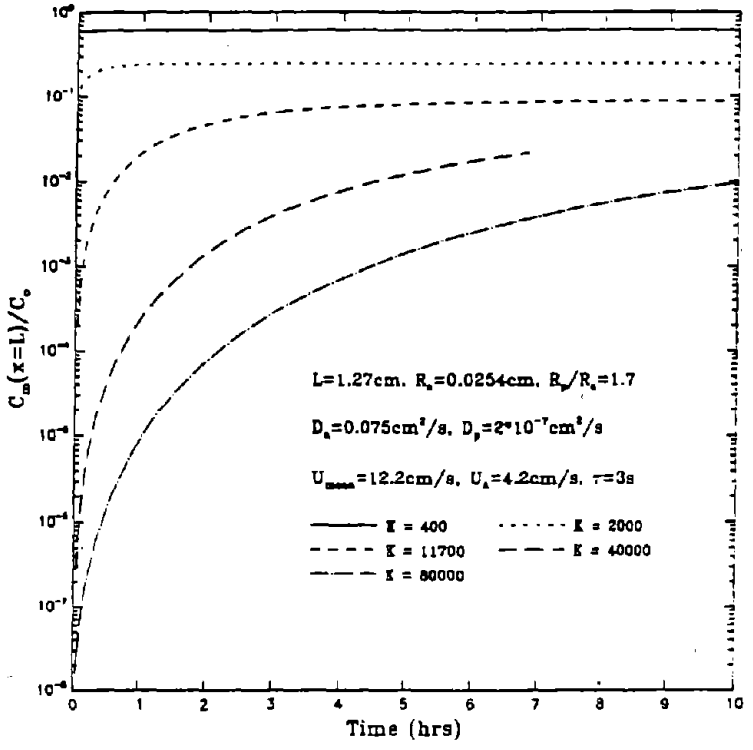

Figure 4: Variation of C_m/C_o with Partition Coefficient.

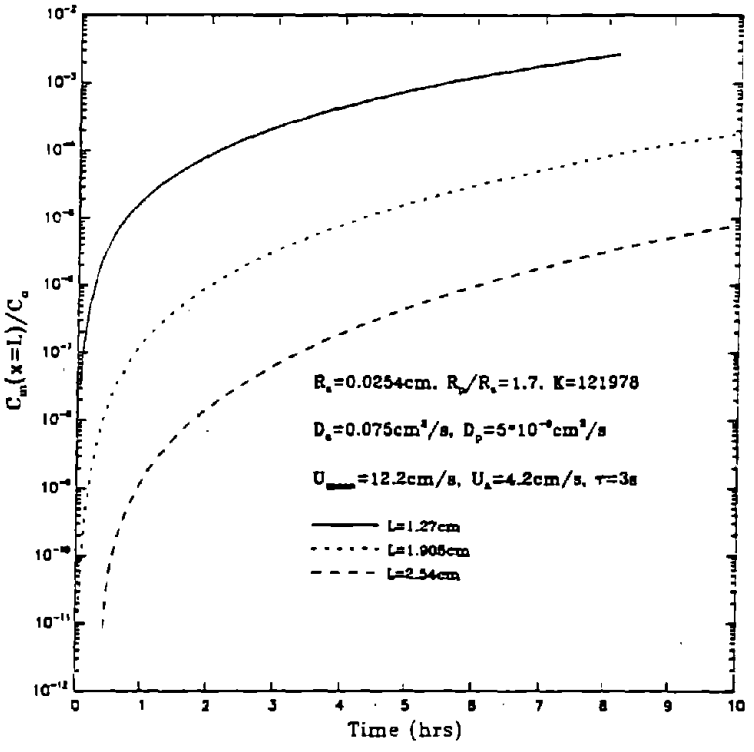

Figure 5: Variation of C_m/C_o with Channel Length.

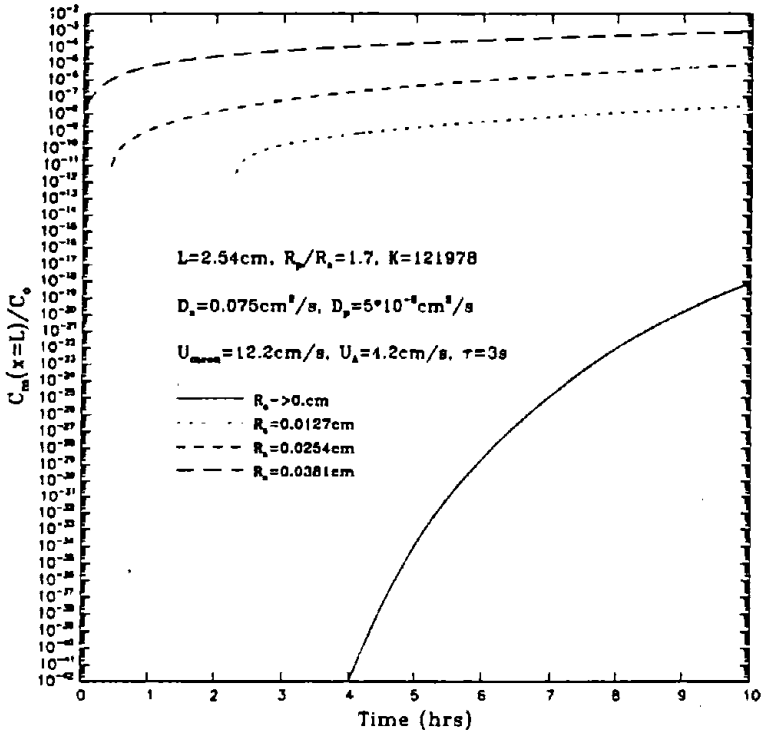

Figure 6: Variation of C_m/C_o with Channel Radius.

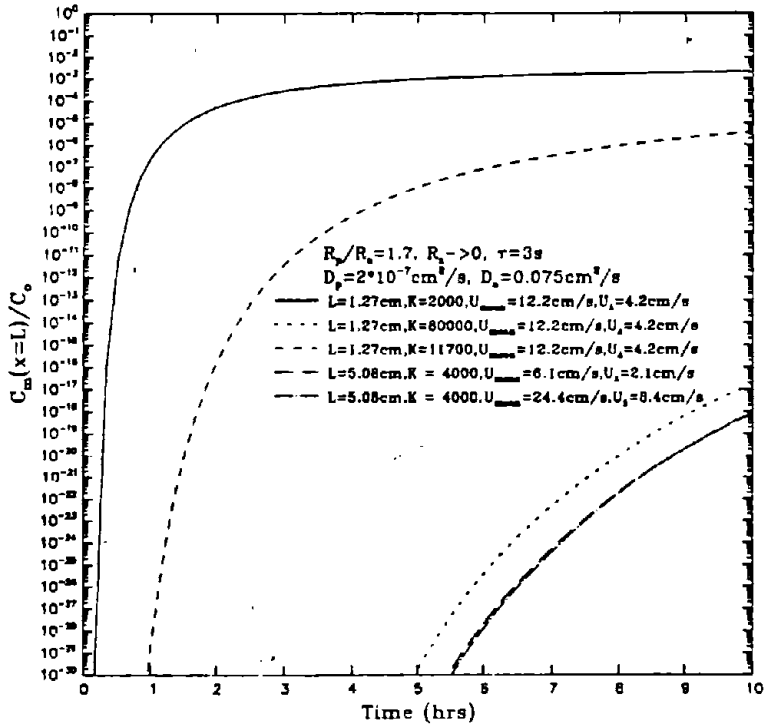

Figure 7: Variation of C_m/C_o with Tube Length and with Partition Coefficient and Apparent Velocity for the Limiting Case R_s = 0.

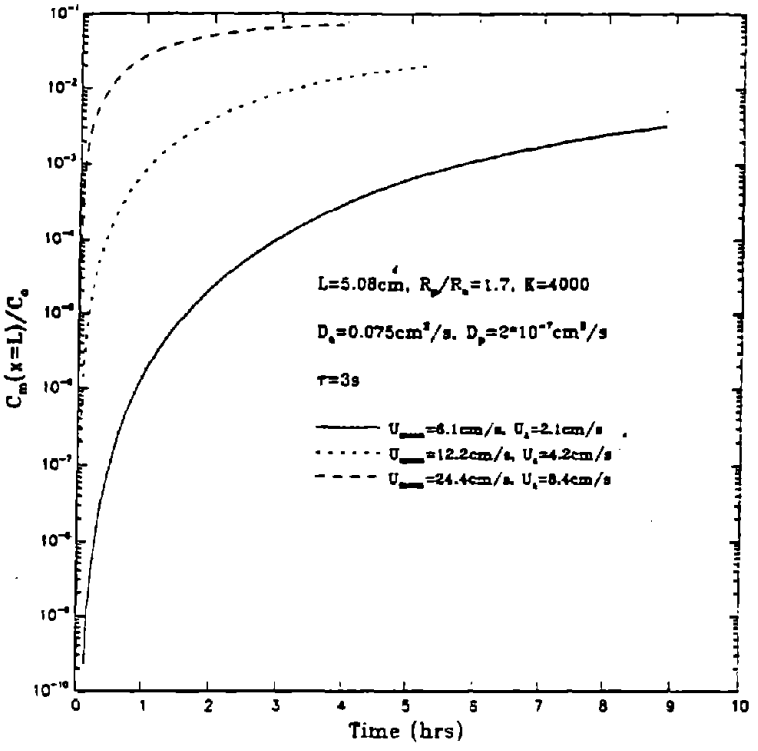

Figure 8: Variation of C_m/C_o with Air Mean Velocity.

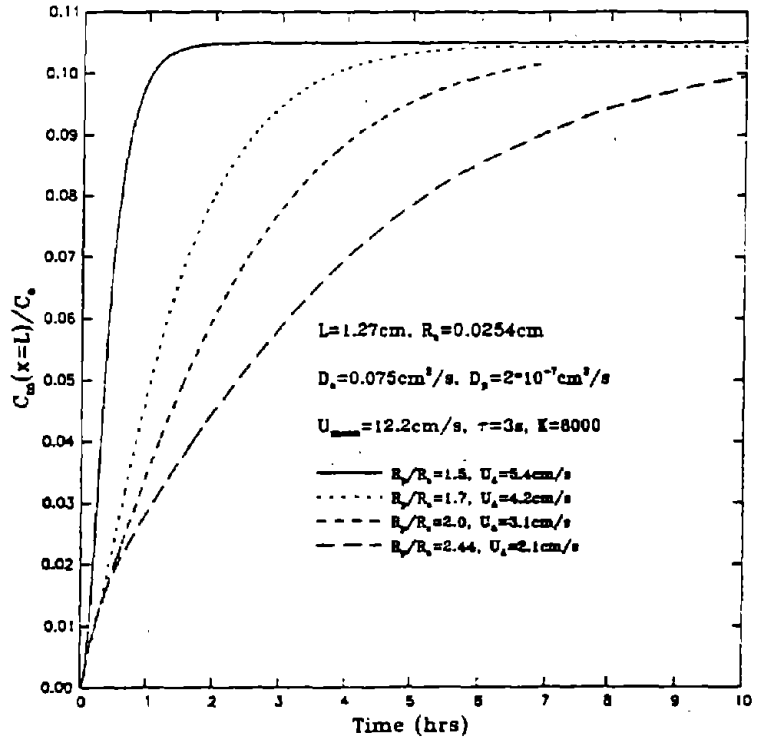

Figure 9: Variation of C_m/C_o with Channel Hole Spacing Characterized by the Ratio R_p/R_s.

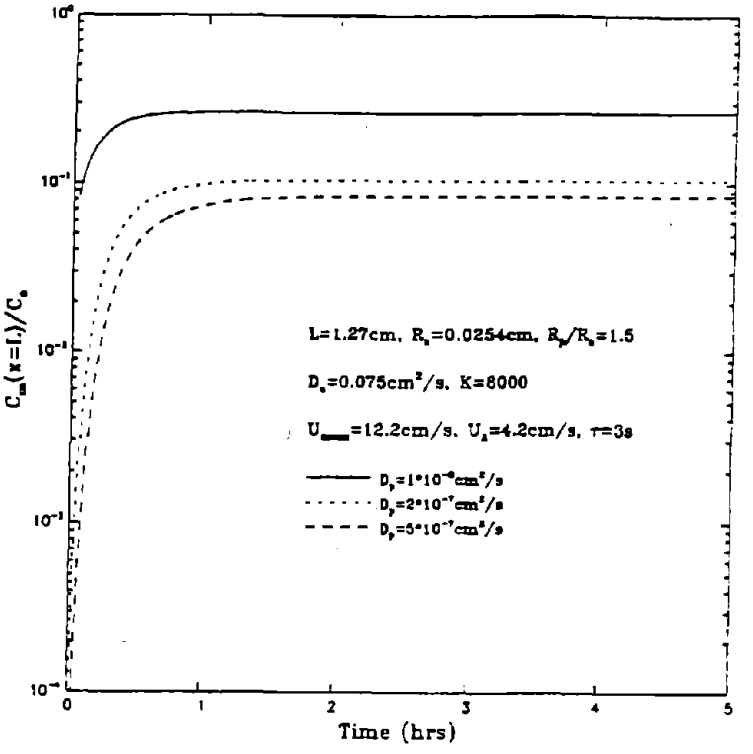

Figure 10: Variation of C_m/C_o with Polymer Diffusivity.

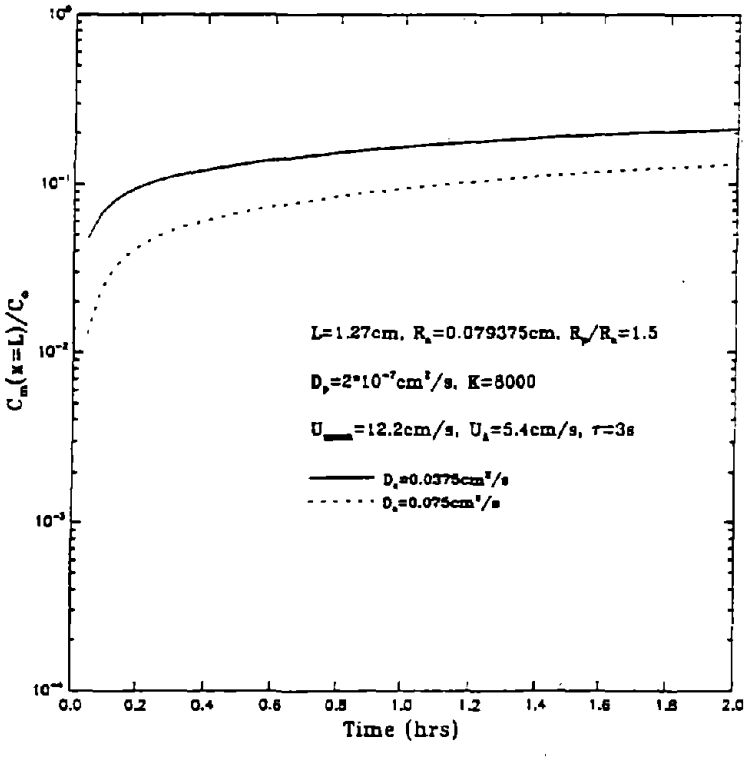

Figure 11: Variation of C_m/C_o with Air Diffusivity.

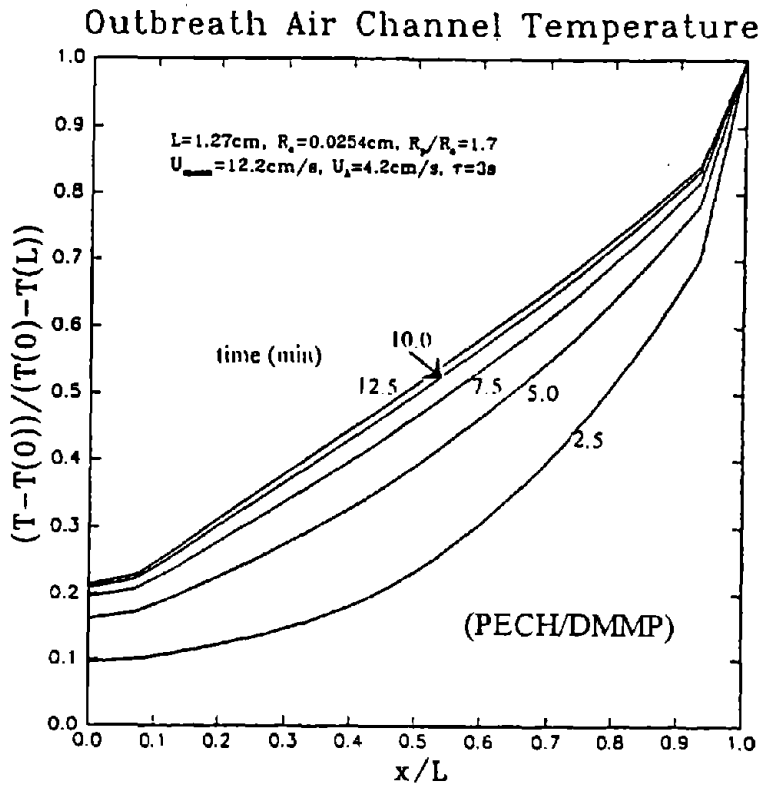

Figure 12: Predicted Temperature Distributions in the Air Channel during Breathing at Selected Times.

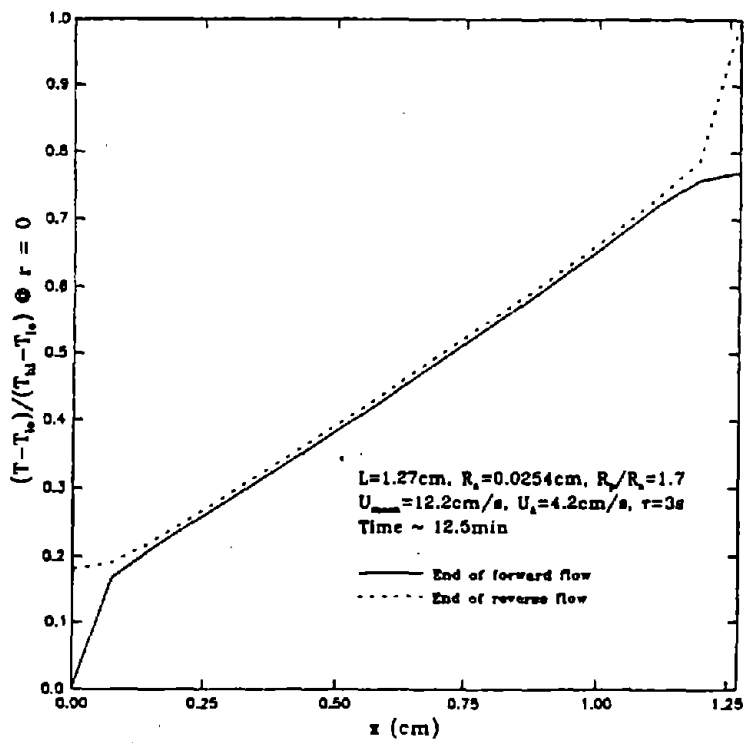

Figure 13: Temperature Distribution Following in and out Breaths after 12.5 Minutes of Respiration.

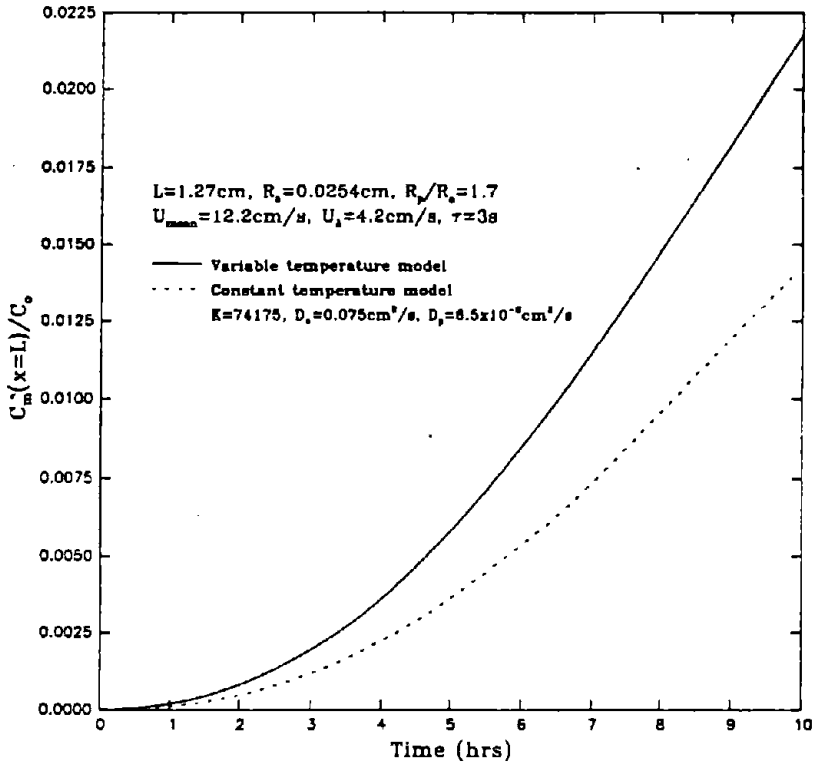

Figure 14: Comparison Between Results Obtained with Temperature Effect Included and Those Using an Average Constant Temperature.

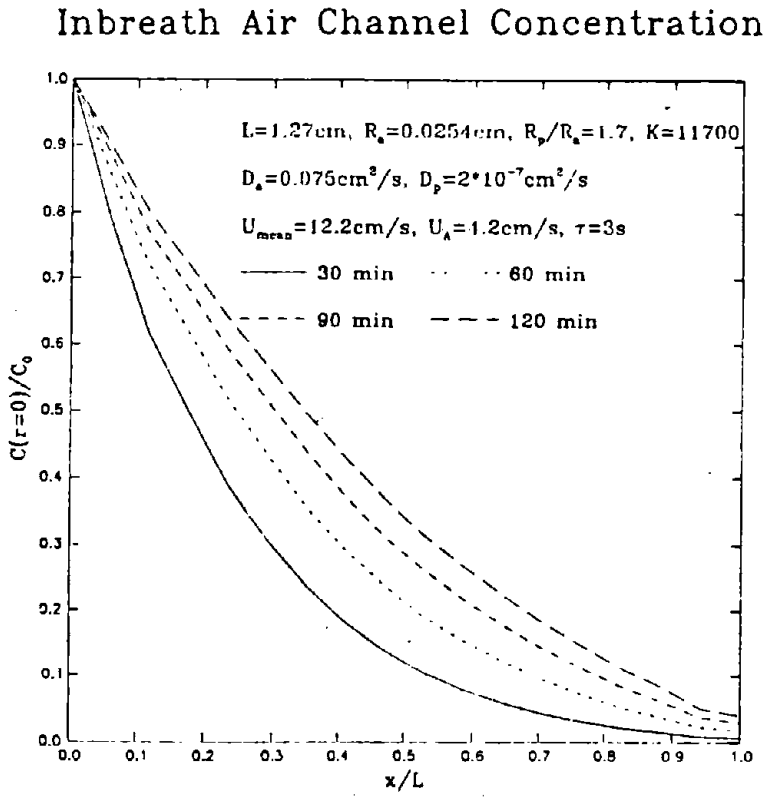

Figure 15: Predicted Concentration Distributions at Selected Times.

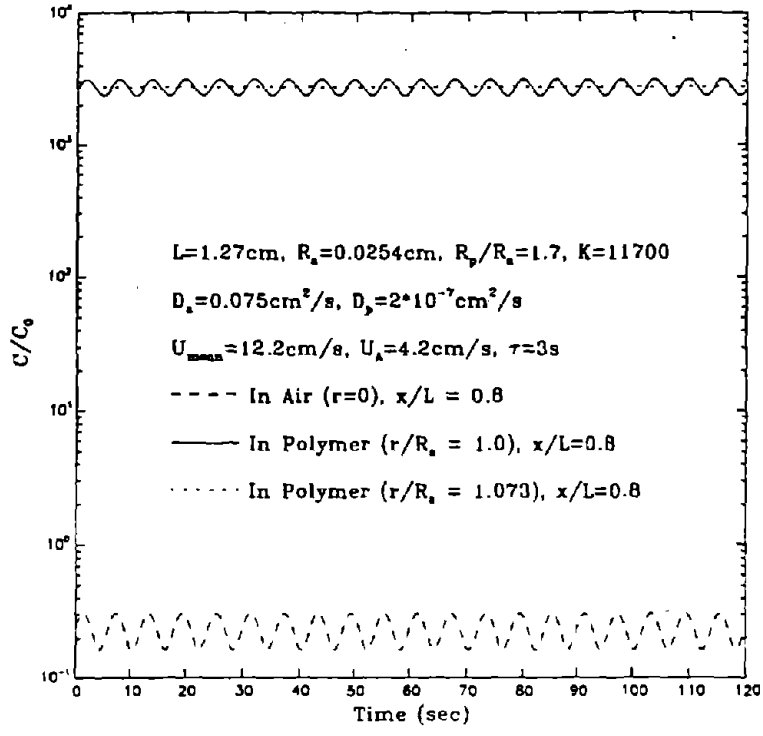

Figure 16: Predicted Cyclic Concentrations After 1 hr. of Breathing.

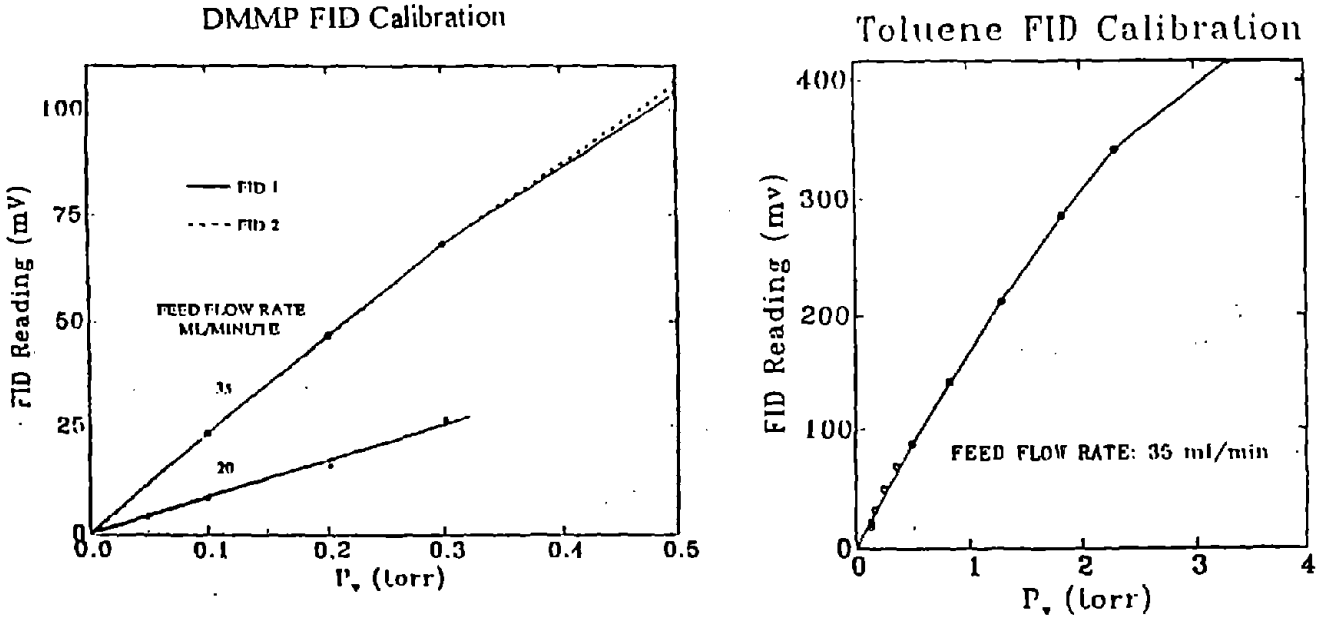

Figure 17: Example of FID Calibration Curves for DMMP and Toluene.

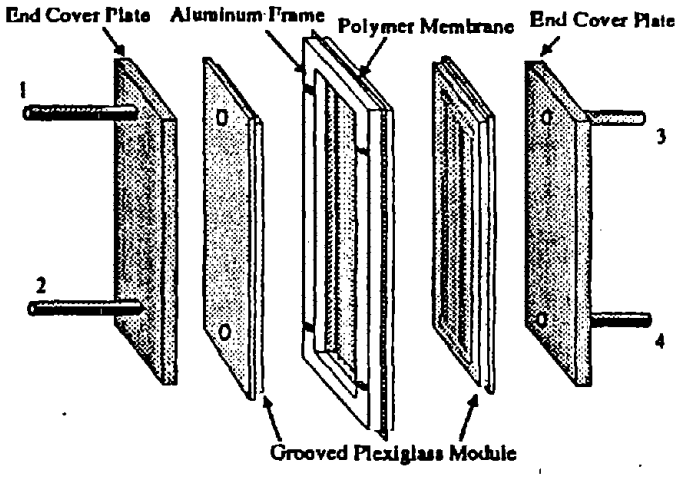

Figure 18: Schematic of Polymer Property Measurement Module.

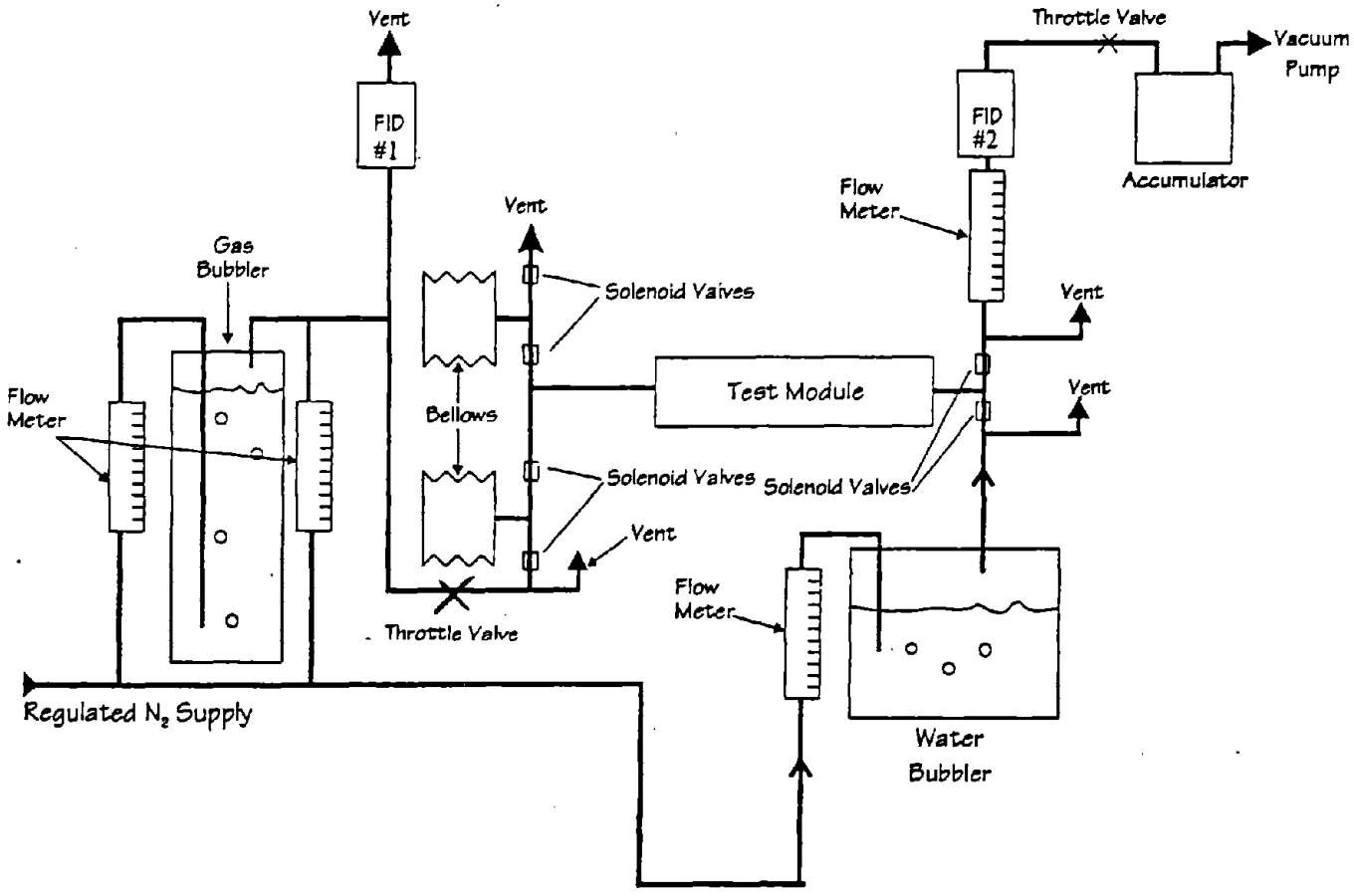

Figure 19: Schematic of Simulated Breathing Test Loop.

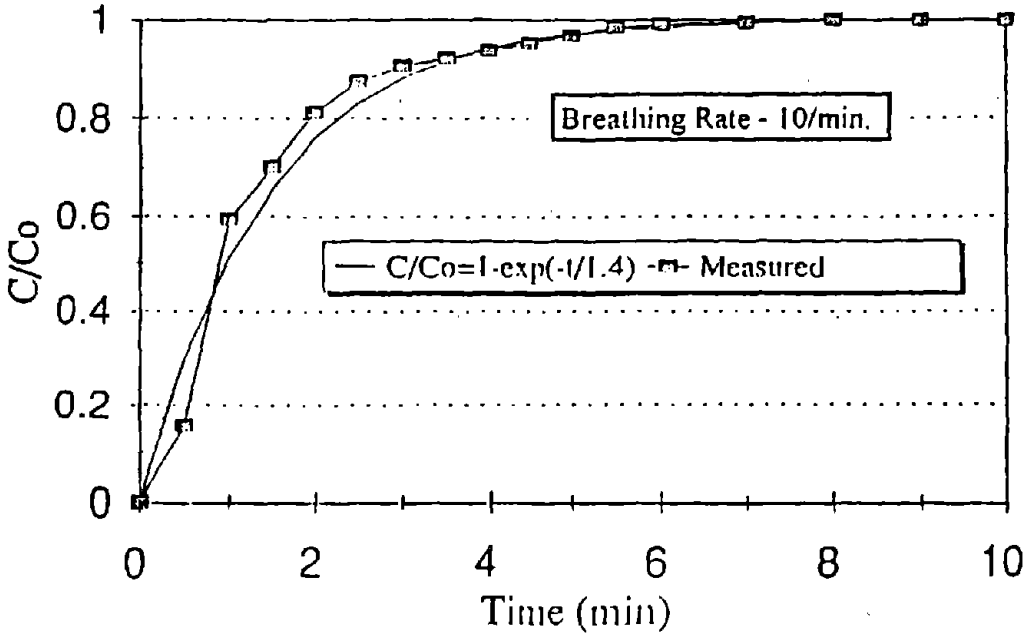

Figure 20: Step Response of Measurement System Showing Lag Due to Lines and FID Compared with Exponential Model with a Time Constant of 1.4 Minutes.

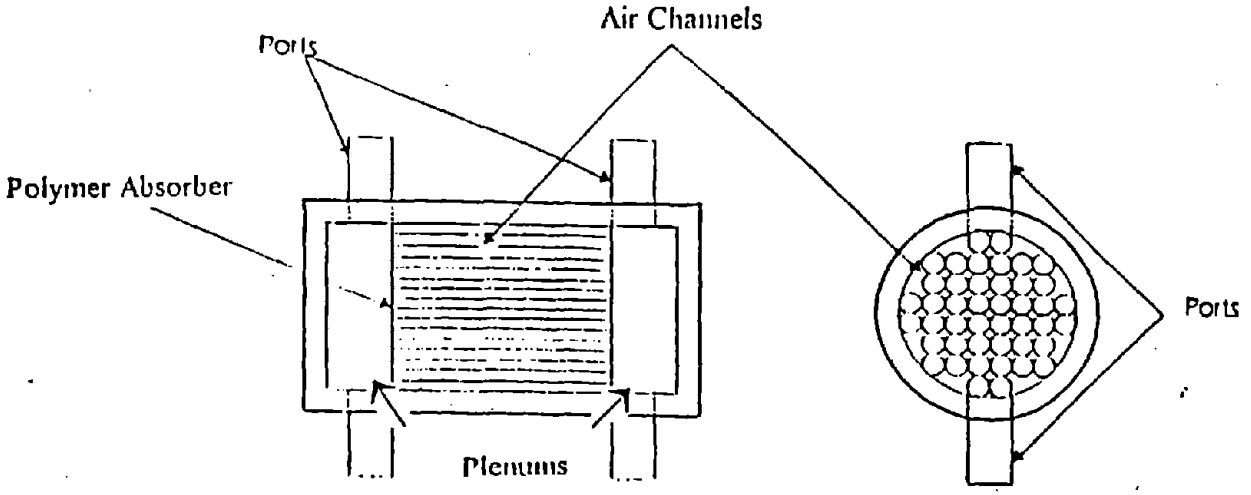

Figure 21: Polymer Absorber Test Module for Simulated Breathing Loop.

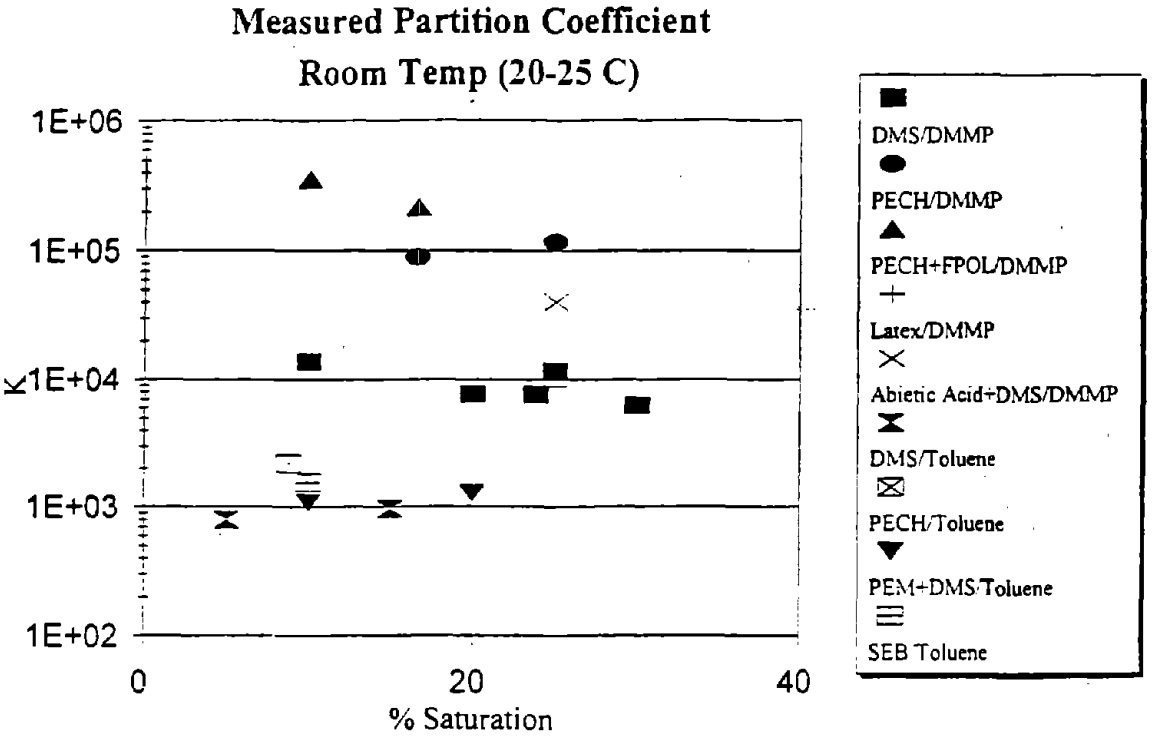

Figure 22: Measured Partition Coefficients as a Function of Concentration.

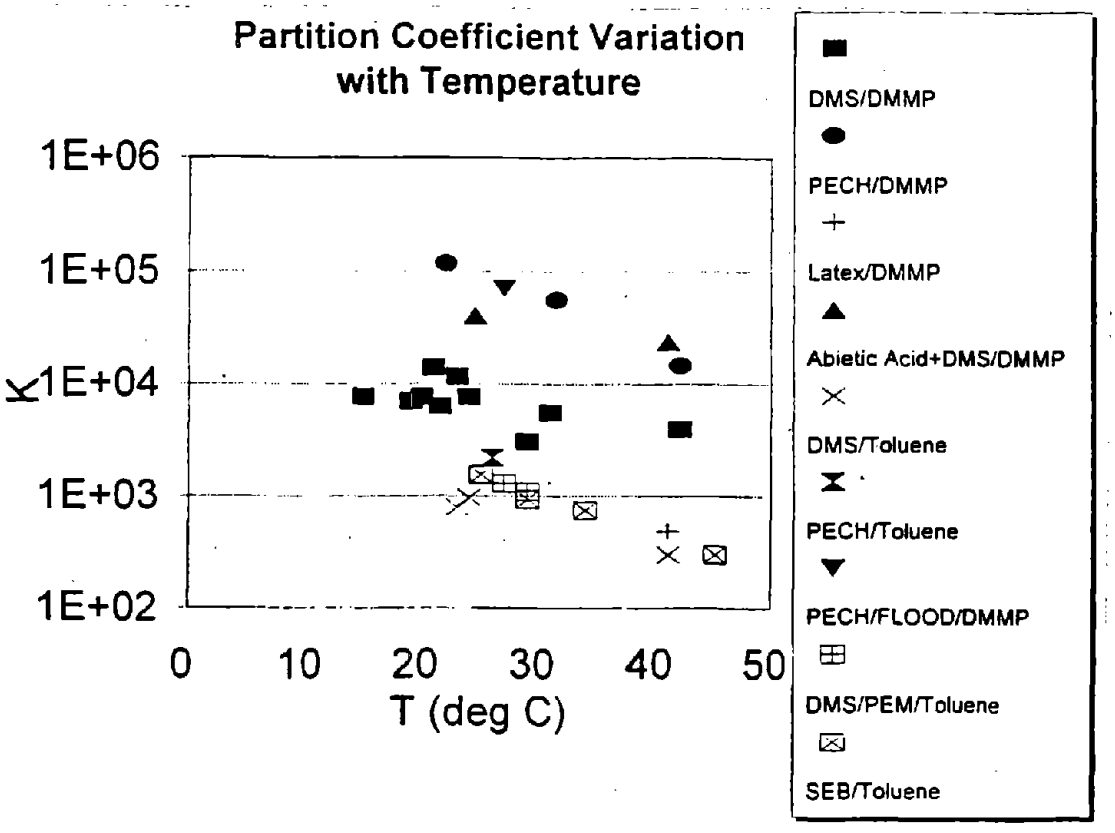

Figure 23: Influence of Temperature on Measured Partition Coefficients.

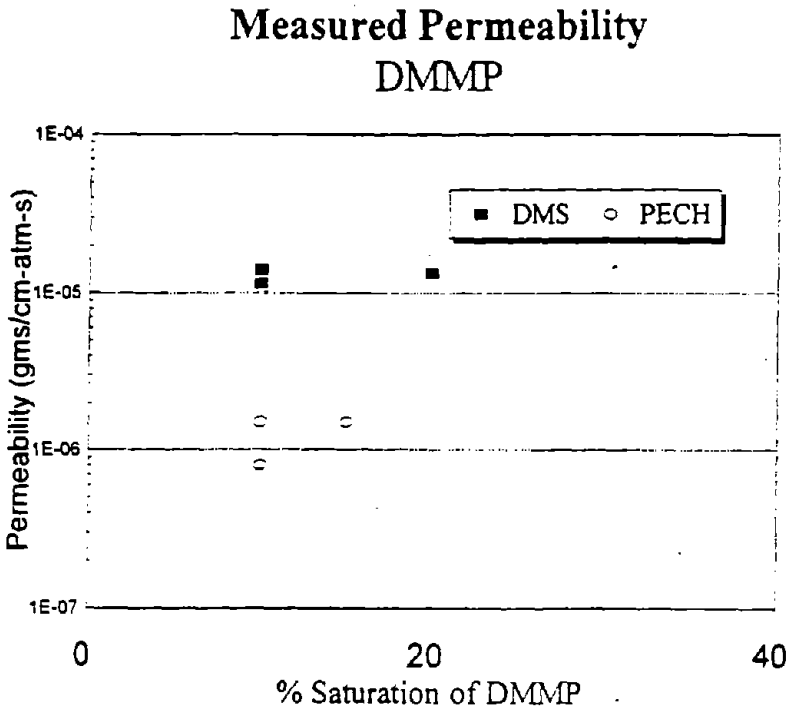

Figure 24: Measured Permeability of DMMP in DMS and PECH.

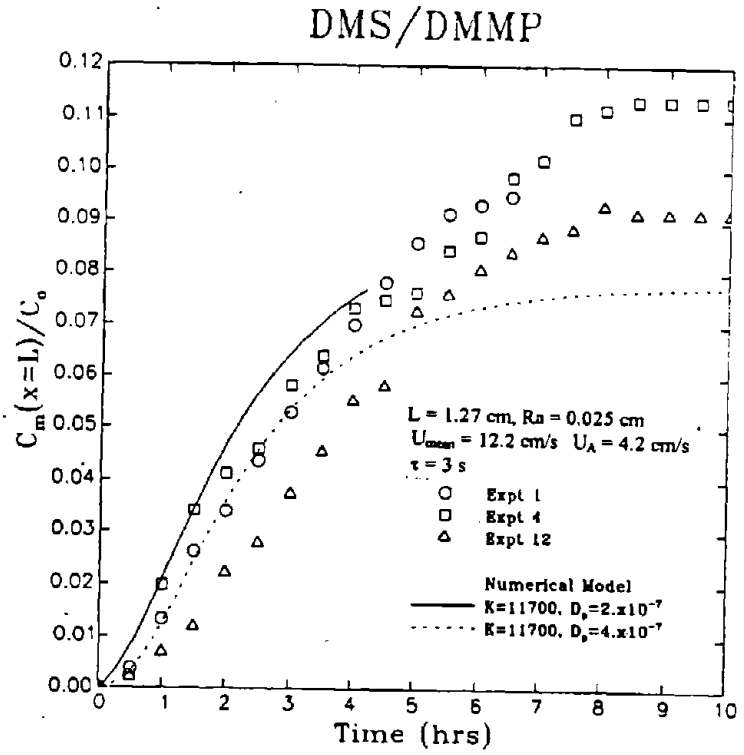

Figure 25: Results of a Simulated Breathing Test Repeated Three Times for a DMMP/DMS Module Showing Data Repeatability and Compared with Numerical Predictions.

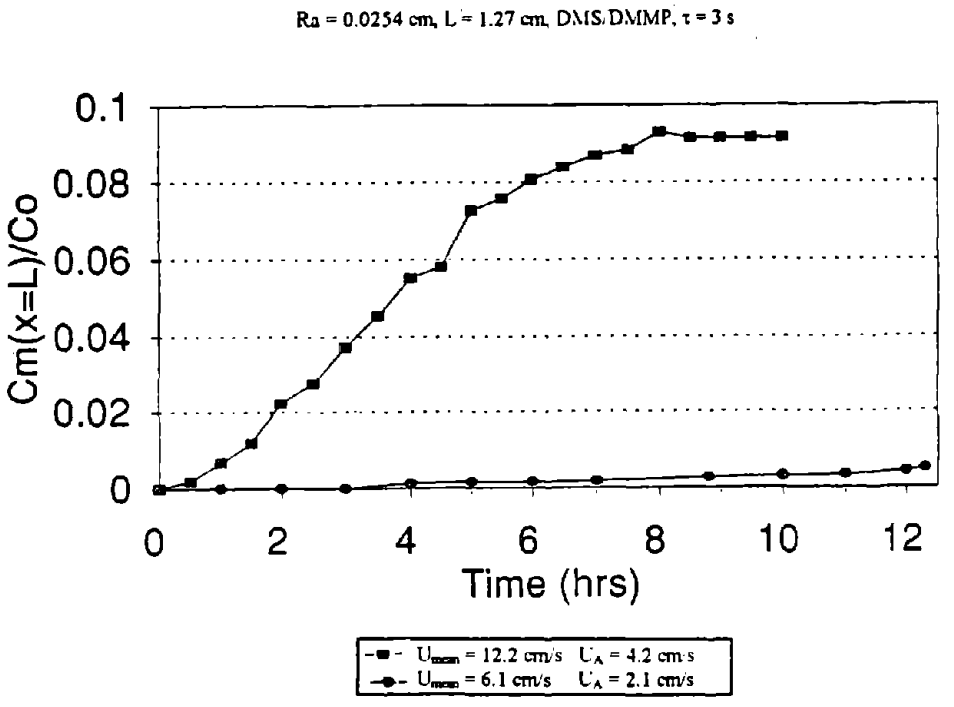

Figure 26: Influence of Velocity on Measured C_m/C_o Values for DMMP/DMS.

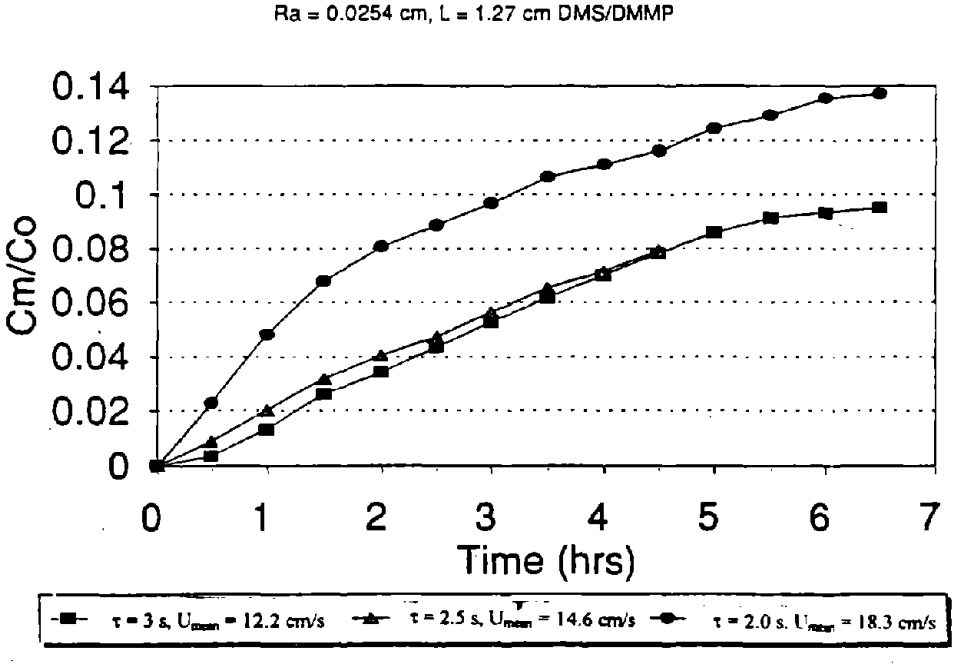

Figure 27: Influence of Breathing Rate on Measured Concentrations for DMMP/DMS.

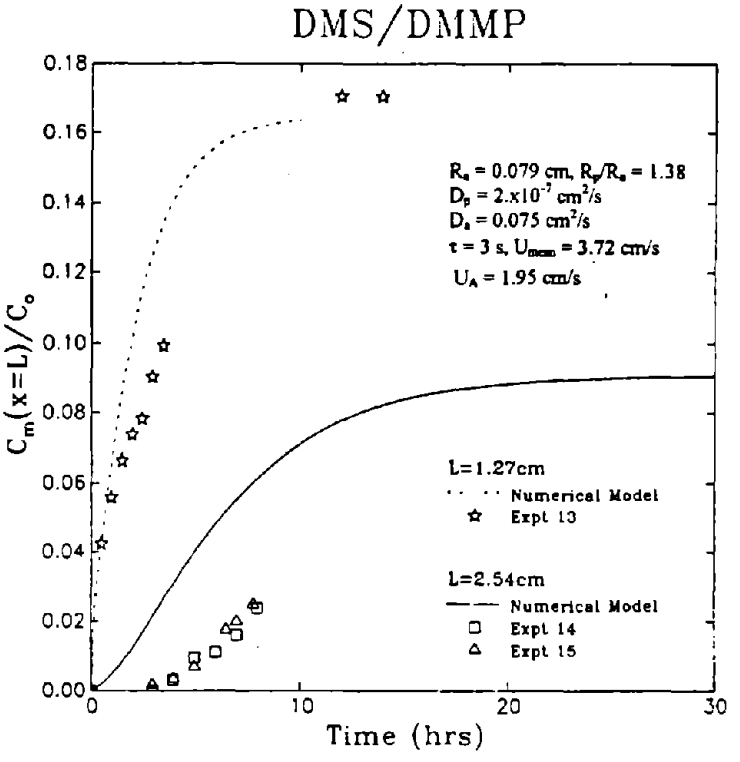

Figure 28: Effect of Module Length. Comparison of Experimental Data and Numerical Predictions for a Factor of two Variation in Length.

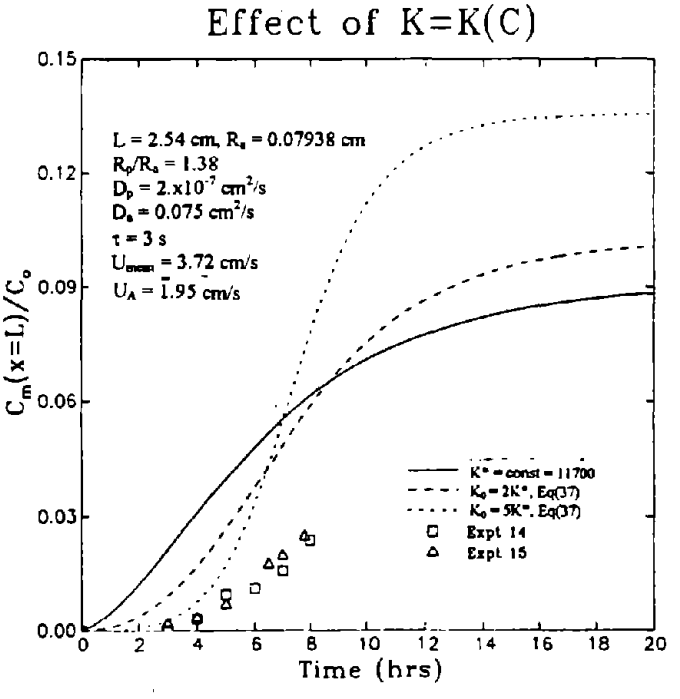

Figure 29: Comparison of Numerical Predictions Employing Concentration Dependent Partition Coefficients with Experimental Data for DMMP/DMS.

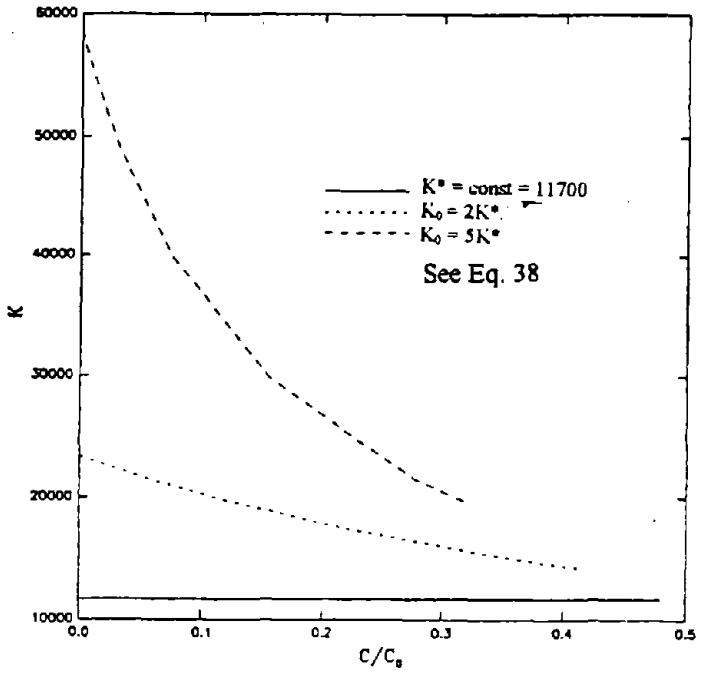

Figure 30: Model for Variation of K with Concentration Selected for Numerical Computations of Figure 29.

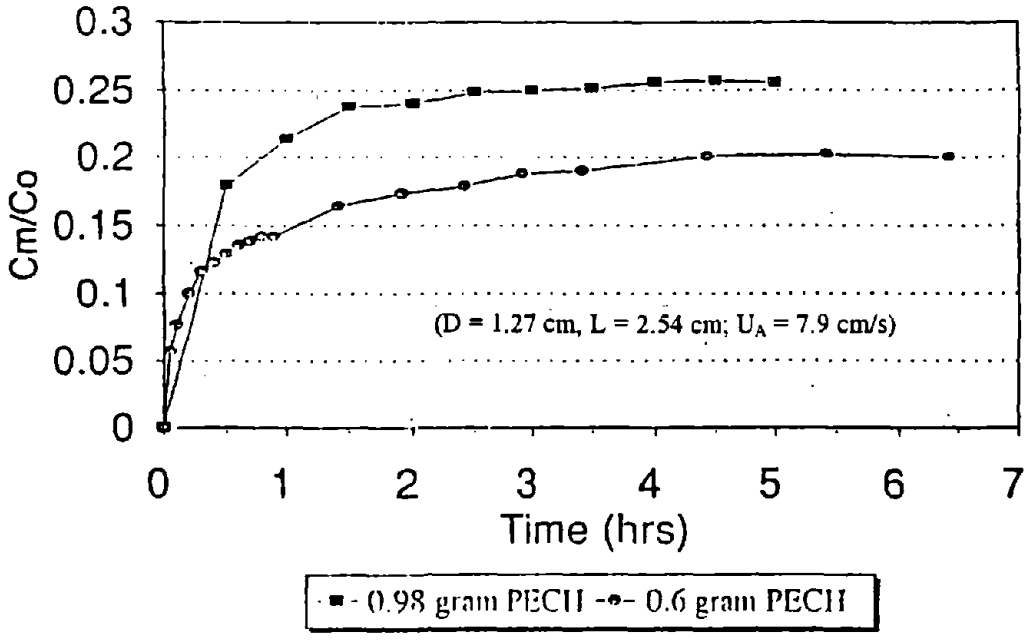

Figure 31: Results of Simulated Breathing Tests of DMMP/PECH Foam Modules. (Precoated Approximate Foam Cell Size = 0.08 cm)

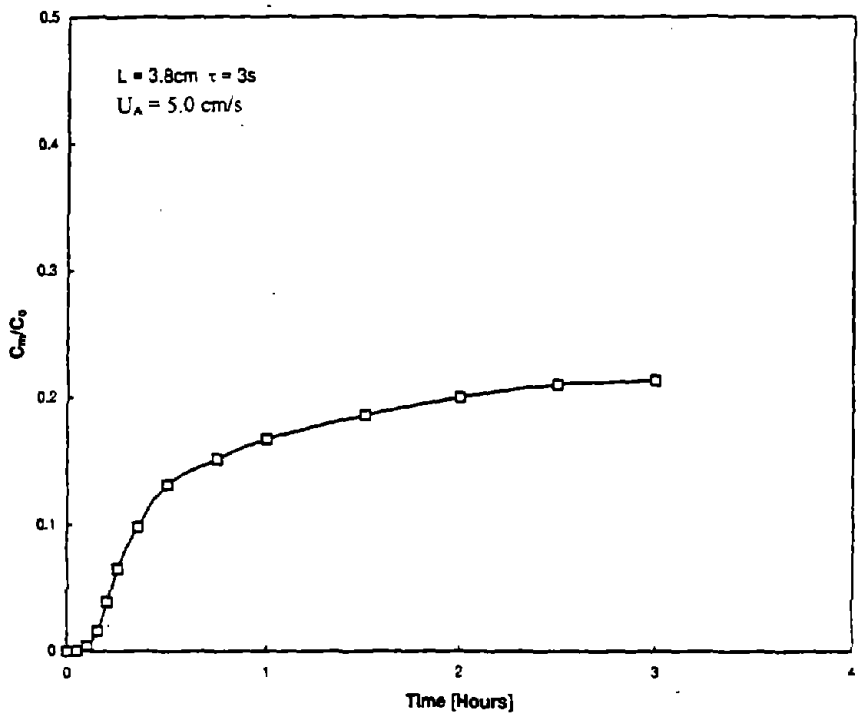

Figure 32: Experimental Result for PECH Rolled-Up Module.

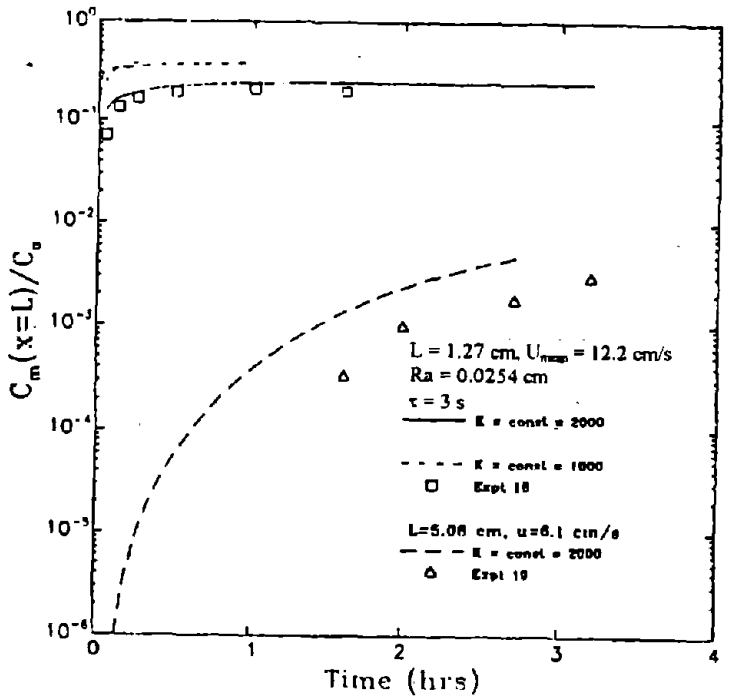

Figure 33: Experimentally Measured Performance of 1.27 and 5.08 cm Long DMS Modules with Toluene. Also Shown are Numerical Predictions for These Cases.

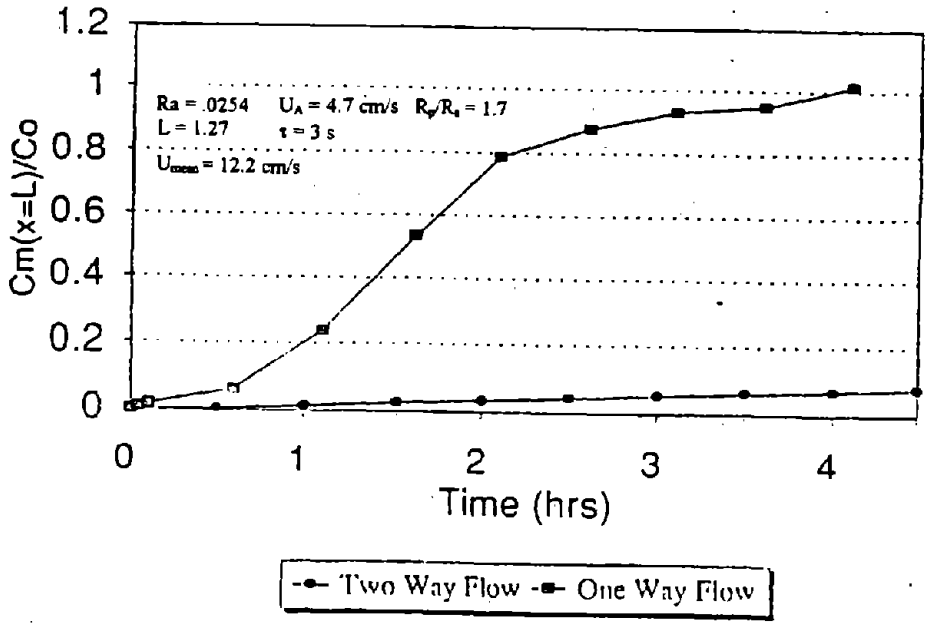

Figure 34: Comparison of Measured Concentrations in Two Way Oscillatory Flow with Those of Conventional One Way Flow.

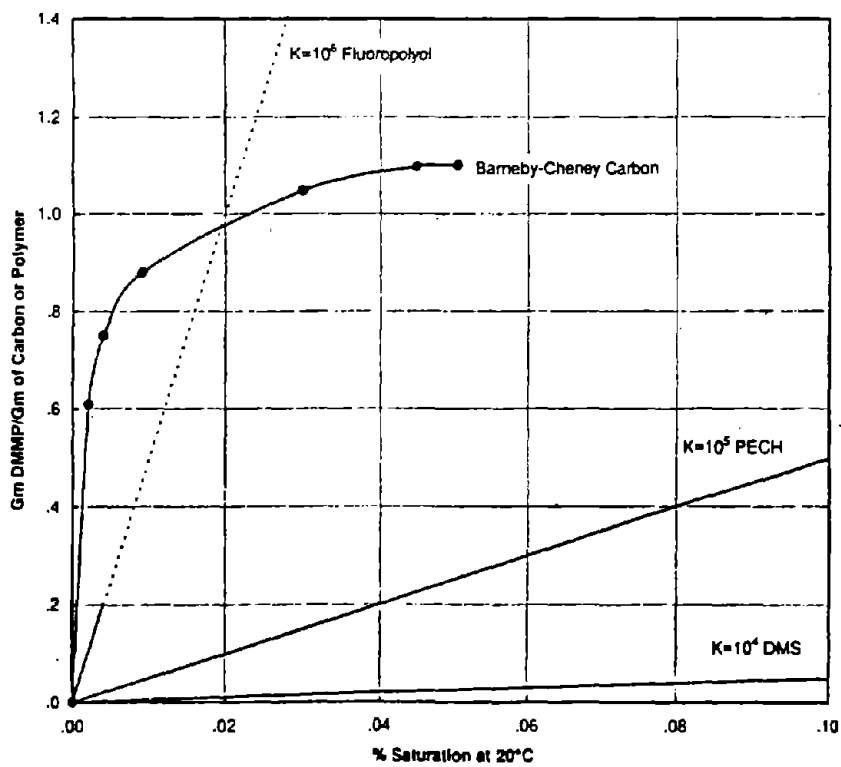

Figure 35: DMMP Concentration Isotherms for Activated Charcoal and Polymers.

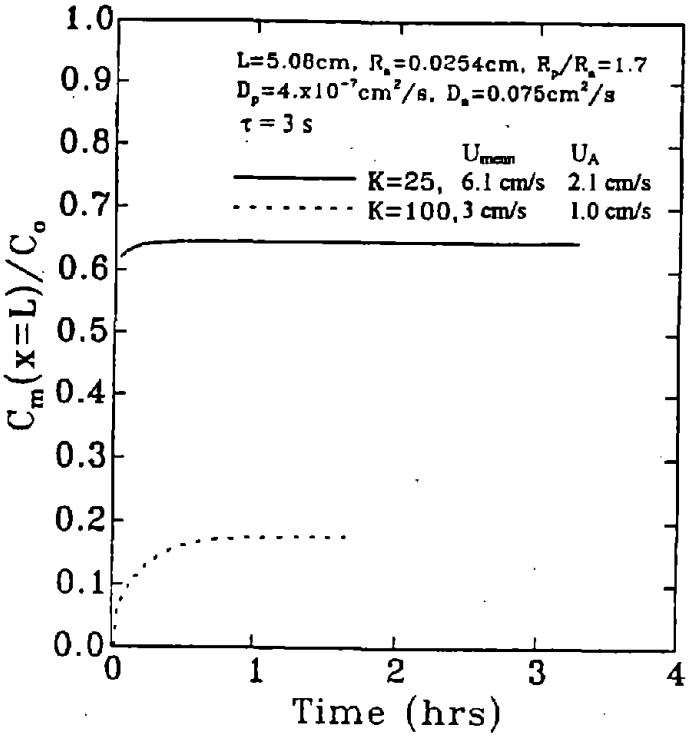

Figure 36: Predicted Performance for Values of K = 25 and 100, Estimated to be Typical of High Vapor Pressure Compounds Such as Methylene Chloride.

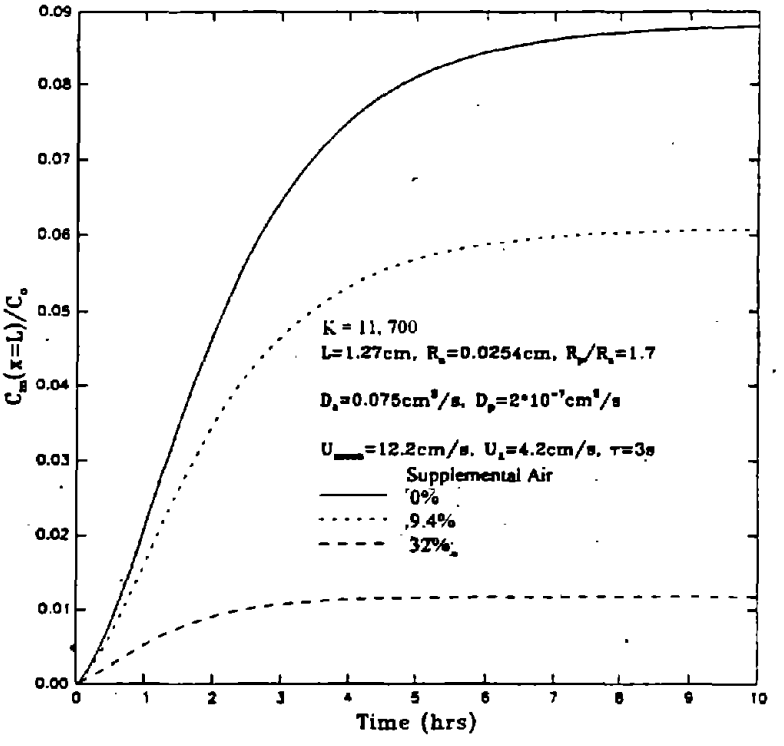

Figure 37: Calculated Effect of Supplemental Air on C_m/C_o.

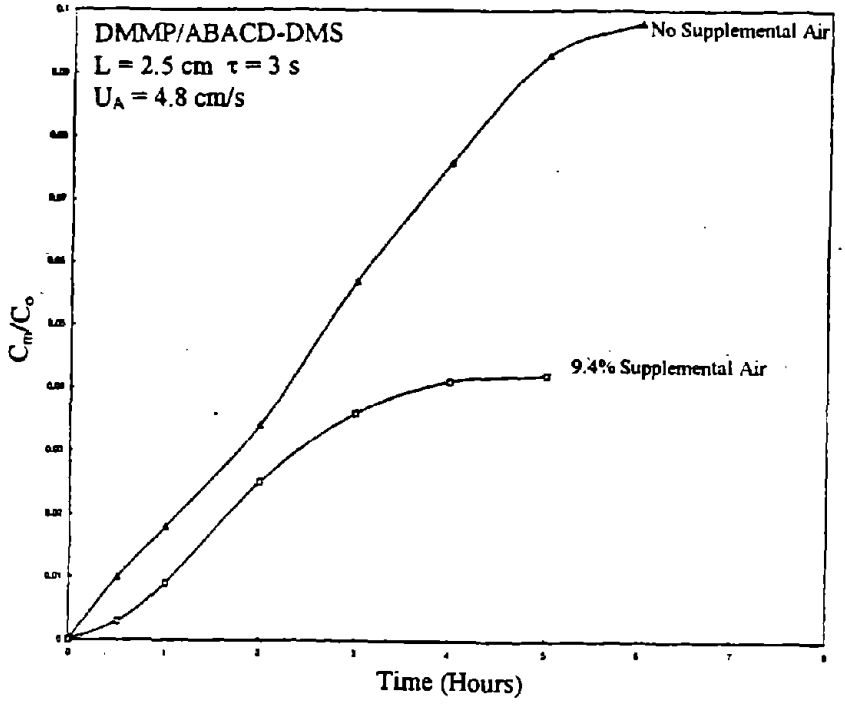

Figure 38: Measured Effect of Supplemental Air on C_m/C_o.

PAPERS BEING SUBMITTED FOR PUBLICATION

1. "Analysis of Mass and Heat Transfer in a Two Way Flow Respirator," *To be submitted to American Industrial Hygiene Association Journal*," K.M. Kalumuck, S. Prabhukumar, and C.E. Brown.

2. "An Experimental Study of Oscillating Flow for Use in Respirators," *To be submitted to Applied Occupational and "Environmental Hygiene*," C.E. Brown, K.M. Kalumuck, and G.S. Frederick.

3. "Note on the Importance of Temperature Gradients on Diffusion in Polymers," *To be submitted to Journal of Polymer Science*, C.E. Brown and K.M. Kalumuck.